

# Finding statistically significant communities in networks

Andrea Lancichinetti,<sup>1,2</sup> Filippo Radicchi,<sup>3</sup> José J. Ramasco,<sup>4,1</sup> and Santo Fortunato<sup>1</sup>

<sup>1</sup>*Complex Networks & Systems Lagrange Laboratory, ISI Foundation, Turin, Italy*

<sup>2</sup>*Department of Physics, Politecnico di Torino, Turin, Italy*

<sup>3</sup>*Amaral Lab, Chemical and Biological Engineering, Northwestern University, Evanston, IL, USA*

<sup>4</sup>*Instituto de Física Interdisciplinar y Sistemas Complejos IFISC (CSIC-UIB), E-07122 Palma de Mallorca, Spain*

Community structure is one of the main structural features of networks, revealing both their internal organization and the similarity of their elementary units. Despite the large variety of methods proposed to detect communities in graphs, there is a big need for multi-purpose techniques, able to handle different types of datasets and the subtleties of community structure. In this paper we present OSLOM (Order Statistics Local Optimization Method), the first method capable to detect clusters in networks accounting for edge directions, edge weights, overlapping communities, hierarchies and community dynamics. It is based on the local optimization of a fitness function expressing the statistical significance of clusters with respect to random fluctuations, which is estimated with tools of Extreme and Order Statistics. OSLOM can be used alone or as a refinement procedure of partitions/covers delivered by other techniques. We have also implemented sequential algorithms combining OSLOM with other fast techniques, so that the community structure of very large networks can be uncovered. Our method has a comparable performance as the best existing algorithms on artificial benchmark graphs. Several applications on real networks are shown as well. OSLOM is implemented in a freely available software (<http://www.oslom.org>), and we believe it will be a valuable tool in the analysis of networks.

PACS numbers: 89.75.Hc

## I. INTRODUCTION

The analysis and modeling of networked datasets are probably the hottest research topics within the modern science of complex systems [1–7]. The main reason is that, despite its simplicity, the network representation can disclose some relevant features of the system at large, involving its structure, its function, as well as the interplay between structure and function. The elementary units of the system are reduced to simple points, called *vertices* (or *nodes*), while their pairwise relationships/interactions are pictured as *edges* (or *links*). It is fairly easy to spot the two main ingredients of a graph in many instances. Therefore networks can be found everywhere: in biology (e. g., proteins and their interactions), ecology (e. g., species and their trophic interactions), society (e. g., people and their acquaintanceships). Other noteworthy examples include the Internet (routers/autonomous systems and their physical and/or wireless connections), the World Wide Web (URLs and their hyperlinks), etc..

The structure of most networks, beneath the intrinsic disorder due to the stochastic character of their generation mechanisms, reveals a high degree of organization. In particular, vertices with similar properties or function have a higher chance to be linked to each other than random pairs of vertices and tend to form highly cohesive subgraphs, which are called *communities* (also *modules* or *clusters*). Examples of communities are groups of mutual acquaintances in social networks [8–10], subsets of Web pages on the same subject [11], compartments in food webs [12, 13], functional modules in protein interaction networks [14], biochemical pathways in metabolic networks [15, 16], etc..

Detecting communities in graphs may help to identify functional subunits of the system and to uncover similarities among vertices that are not apparent in the absence of detailed (non-topological) information. Vertices belonging to the same community may be classified according to their structural position within the cluster, which may be correlated to their role. Vertices in the core of the cluster may have a function of control and stability within the module, whereas boundary vertices are likely to be mediators between different parts of the graph. The community structure of a network can also be a powerful visual representation of the system: instead of visualizing all the vertices and edges of the network (which is impossible on large systems), one could display its communities and their mutual connections, obtaining a far more compact and understandable description of the graph as a whole. It is thus not surprising that community detection in graphs has been so extensively investigated over the last few years [17]. A huge variety of different methods have been designed by a truly interdisciplinary community of scholars, including physicists, computer scientists, mathematicians, biologists, engineers and social scientists.

However, most algorithms currently available cannot handle important network features. Many methods are designed to find clusters in undirected graphs, and cannot be easily (or not at all) extended to directed graphs. However, there are many datasets for which edge directedness is an essential feature. Citation networks, food webs and the Web graph are but a few examples. Similar problems arise when edges carry weights, indicating the strength of the interaction/affinity between vertices, although extensions are generally easier in this case.

Likewise, the great majority of algorithms are not ca-

pable to deal with the peculiar features of community structure. For example, each vertex is typically assigned to a single cluster, while in several instances, like in social networks, vertices are typically shared between two or more clusters. In such cases communities are *overlapping* (and partitions become *covers*) and very few methods account for this possibility [18–25], which considerably increases the complexity of the problem. Furthermore, community structure is very often *hierarchical*, i.e. it consists of communities which include (or are included by) other communities. Hierarchies are common in human societies and are crucial for an efficient management of large organizations. Simon pointed out that hierarchy gives robustness and stability to complex systems, yielding an evolutionary advantage on the long run [26]. However, most community finding methods typically look for the “best” partition of a network, disregarding the possible existence of hierarchical structure. Instead, a method should be able to recognize if there is hierarchical structure and, if yes, identify the corresponding levels [27–29].

It is also very important for a method to distinguish communities from pseudo-communities. The existence of clusters indicate a preference by some groups of vertices to link to each other. But, if the linking probability is the same for all pairs of vertices, like in random graphs, no communities are expected. In this case, concentrations of edges within groups of vertices are simply the result of random fluctuations, they do not represent potentially non-trivial structures. Many algorithms are not able to see this difference and find clusters in random graphs as well, although they are not meaningful. Scholars have just begun to assess the issue of significance of clusters [30, 31].

Finally, given the recent availability of time-stamped networked datasets, it is now possible to carry out quantitative studies on the dynamics of community structure, about which very little is known [32–37]. A simple way to treat dynamic datasets is to analyze snapshots of the system at different times separately, and then map communities of different snapshots onto each other, such that one can follow the dynamic of each cluster in time. However, focusing on individual snapshots means disregarding the information on the system at previous times. Ideally a partition/cover of the system at time  $t$  should be faithful both to its structure at time  $t$  and to its history [34, 37].

In this paper we propose the first method able to meet all requirements listed above, the Order Statistics Local Optimization Method (OSLOM). It is a method that optimizes locally the statistical significance of clusters, defined with respect to a global null model. The concept of statistical significance is inspired by recent work of some of the authors [31, 38]. The paper is structured as follows. After introducing the method, we test its performance on artificial benchmark graphs, comparing it with the performances of the best algorithms currently available. Next, we pass to the analysis of real networks, followed by a final discussion on the work. Some of the

tests on artificial and real networks are reported in the Appendix.

## II. METHODS

### A. Statistical significance of clusters

In this section we explain how to estimate the statistical significance of a given cluster. OSLOM will use the significance as a fitness measure in order to evaluate the clusters. Following our previous work [31], we define it as the probability of finding the cluster in a random null model, i. e. in a class of graphs without community structure. We choose the configuration model [39] as our null model. This is a model designed to build random networks with a given distribution of the number of neighbors of a vertex (degree). The networks are generated by joining randomly vertices under the constraint that each vertex has a fixed number of neighbors, taken from the pre-assigned degree distribution. This is basically the same null model adopted by Newman and Girvan to define modularity [40].

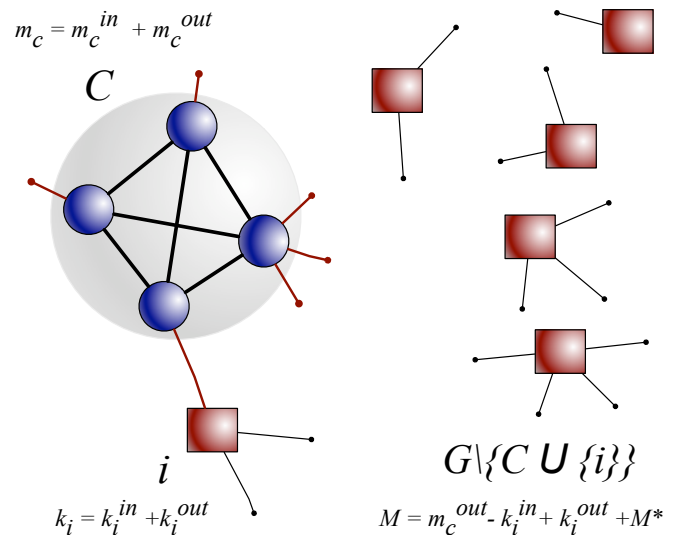


Figure 1: A schematic representation of a subgraph  $C$ , whose significance is to be assessed. The subgraph  $C$  is embedded within a random graph generated by the configuration model. The degrees of all vertices of the network are fixed, in the figure we have highlighted the degrees of  $C$  ( $m_c$ ), of the vertex  $i$  at the center of the analysis ( $k_i$ ) and of the rest of the graph  $G \setminus [C \cup \{i\}]$  ( $M$ ). These quantities are expressed as sums of contributions which are internal to their own set of vertices (as  $M^*$ ) or related to subgraph  $C$  (in or out). This notation is used in the distribution of Eq. 1.

We start from a graph  $\mathcal{G}$  with  $N$  vertices and  $E$  edges. The framework for the analysis is sketched in Fig. 1. We are given a subgraph  $C$ , whose significance is to be assessed, a vertex  $i \notin C$  and the degree of the vertices

of the rest of the graph  $\mathcal{G} \setminus [\mathcal{C} \cup \{i\}]$ . The degree of subgraph  $\mathcal{C}$  is  $m_{\mathcal{C}}$ ,  $k_i$  is the degree of  $i$ , and the rest of vertices have a total degree  $M$ . We can separate the above quantities in the contributions internal or external to  $\mathcal{C}$  ( $m_{\mathcal{C}}^{in}, m_{\mathcal{C}}^{out}, k_i^{in}$  and  $k_i^{out}$ ); the internal degree of  $\mathcal{G} \setminus [\mathcal{C} \cup \{i\}]$  is  $M^*$  (Fig. 1).

Let us suppose that  $\mathcal{C}$  is a subgraph of graphs generated by the configuration model, where each vertex maintains the degree it has on the graph  $\mathcal{G}$  at study. We assume that the internal degree  $m_{\mathcal{C}}^{in}$  of the subgraph is fixed. If all the other edges of the network are randomly drawn, the probability that  $i$  has  $k_i^{in}$  neighbors in  $\mathcal{C}$  can be written as [38]

$$p(k_i^{in}|i, \mathcal{C}, \mathcal{G}) = A \frac{2^{-k_i^{in}}}{k_i^{out}! k_i^{in}! (m_{\mathcal{C}}^{out} - k_i^{in})! (M^*/2)!}. \quad (1)$$

This equation enumerates the possible configurations of the network with  $k_i^{in}$  connections between  $i$  and  $\mathcal{C}$ . The factorials of the formula express the multiplicity of configurations with fixed values of  $k_i^{in}$ ,  $k_i^{out}$ ,  $(m_{\mathcal{C}}^{out} - k_i^{in})$  and  $M^*/2$ , whereas the power of 2 in the numerator stays for the multiplicity coming from the permutation of the extremes of edges lying between  $i$  and  $\mathcal{C}$ . Several of the terms in the expression can actually be written as a function of constants and  $k_i^{in}$ , such as  $k_i^{out} = k_i - k_i^{in}$  and  $M^* = 2E - m_{\mathcal{C}} - m_{\mathcal{C}}^{out} - 2k_i + 2k_i^{in}$ . The normalization factor  $A$  includes terms not depending on  $k_i^{in}$  and ensures that

$$\sum_{k_i^{in}: M^* \geq 0} p(k_i^{in}|i, \mathcal{C}, \mathcal{G}) = 1. \quad (2)$$

Further details on the numerical implementation of the formula in Eq. 1, as well as on the different approximations taken and their limits, are included in Appendix A.

The probability of Eq. 1 provides a tool to rank the vertices external to  $\mathcal{C}$  according to the likelihood of their topological relation with the group. If vertex  $i$  shares many more edges with the vertices of subgraph  $\mathcal{C}$  than expected in the null model, we could consider the inclusion of  $i$  in  $\mathcal{C}$ , since the relationship between  $i$  and  $\mathcal{C}$  is “unexpectedly” strong. In order to perform the ranking the cumulative probability  $r(k_i^{in}) = \sum_{j=k_i^{in}}^{k_i} p(j|i, \mathcal{C}, \mathcal{G})$  of having a number of internal connections equal or larger than  $k_i^{in}$  is estimated, following Ref. [31]. Given that the vertex degree is a discrete variable, the cumulative distribution has a specific step-wise profile for each value of  $k_i$ . In order to facilitate the comparison of vertices with different degrees, we implement a bootstrap strategy by assigning to each vertex  $i$  a value of  $r$ ,  $r_i$ , randomly drawn from the interval  $[r(k_i^{in}), r(k_i^{in} + 1)]$ . This choice is important for a meaningful estimate of the clusters’ significance; other options (e. g., taking the middle points of the interval) could lead to the identification of meaningful clusters in random graphs. The bootstrap introduces a stochastic element in the assessment procedure, which will, in turn, lead to the use of Monte Carlo techniques.

The variable  $r$  bears the information regarding the likelihood of the topological relation of each vertex with  $\mathcal{C}$  and has an important feature: it is a uniform random variable distributed between zero and one for vertices of our null model graphs. Calculating its order statistic distributions is thus a relatively easy task. The first candidate among the external vertices to be part of  $\mathcal{C}$  is the vertex with the lowest value of  $r$ , that we indicate  $r_1$ . The cumulative distribution of  $r_1$  in the null model is then given by

$$\Omega_1(r) = P(r_1 < r) = 1 - (1 - r)^{N - n_{\mathcal{C}}}, \quad (3)$$

where  $n_{\mathcal{C}}$  is the number of vertices in  $\mathcal{C}$ . In general, let  $r_q$  be the value of variable  $r$  with rank  $q$  (in increasing order of the variable  $r$ ).

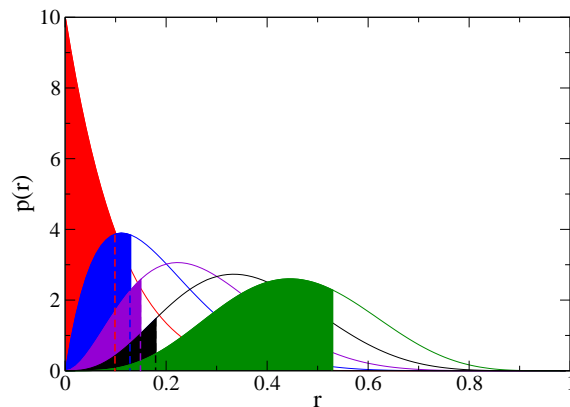


Figure 2: Probability distributions of the scores  $r$  of vertices external to a given subgraph  $\mathcal{C}$  of the graph. The score  $r_q$  is the  $q$ -th smallest score of the external vertices. In this particular case there are 10 external vertices. In the figure, we plot  $p(r_1)$ ,  $p(r_2)$ ,  $p(r_3)$ ,  $p(r_4)$ ,  $p(r_5)$  (from left to right). As an example, the shaded areas show the cumulative probability  $\Omega_q$  for a few values of  $r$  that would correspond to the values estimated in a practical situation. In this case, the black area,  $q = 4$ , is the least extensive and so  $c_m = \Omega_4$ . If  $\phi(c_m) < P$ , the vertices with scores  $r_1, r_2, r_3$  and  $r_4$  will be added to  $\mathcal{C}$ .

Its cumulative distribution is (Fig. 2):

$$\Omega_q(r) = p(r_q < x) = \sum_{i=q}^{N - n_{\mathcal{C}}} \binom{N - n_{\mathcal{C}}}{i} x^i (1 - x)^{N - n_{\mathcal{C}} - i}. \quad (4)$$

The reason for the use of order statistics is that we assume that clustering methods tend to include in each community those vertices which are most strongly connected to vertices of the community. Due to correlations (the vertices in the clusters tend to be connected), we cannot calculate the statistics of the internal connections to the clusters, but we can do it safely for the external vertices. The values of the different  $\Omega_q$  inform us of

how much the external vertices of a group are compatible with the statistics expected in the null model. To evaluate the full group, we define  $c_m = \min_q \{\Omega_q(r_q)\}$  among all the neighbors of  $\mathcal{C}$ , where  $r_q$  are their corresponding ranked values for the  $r$  variable. The distribution of  $c_m$  can be easily tabulated numerically since it only depends on  $N - n_{\mathcal{C}}$ . The cumulative distribution will be denoted as  $P(c_m < x) = \phi(x, N - n_{\mathcal{C}})$ . In the following, we call  $\phi(c_m, N - n_{\mathcal{C}})$  the *score* of the cluster  $\mathcal{C}$ .

## B. Single cluster analysis

Now that a score to evaluate the statistical significance of the clusters has been introduced, the next step is to optimize the score across the network by dividing it into proper clusters. We describe first the optimization of a single cluster score and will extend later the method to deal with the full network. First of all one has to give the method a certain tolerance, in the following referred to as  $P$ . This parameter establishes when a given value of the score is considered significant. Our procedure consists of two phases: first, we explore the possibility of adding external vertices to the subgraph  $\mathcal{C}$ ; second, non-significant vertices in  $\mathcal{C}$  are pruned. They are described below and illustrated schematically in Fig. 3.

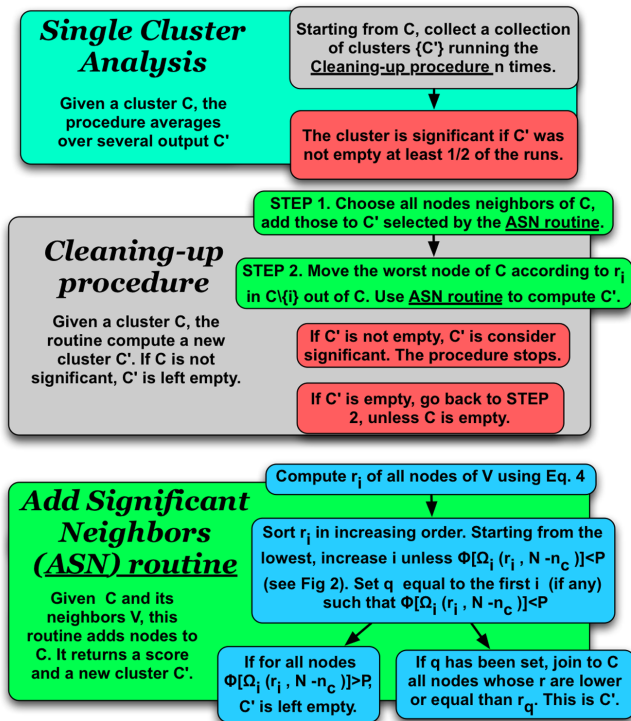


Figure 3: Schematic diagram of the single cluster analysis.

1. For each vertex  $i$  outside  $\mathcal{C}$  and connected to it by at least one edge the variable  $r$  is computed.

Then we calculate  $\Omega_1(r)$  for the vertex with the smallest  $r$ , by using Eq. 3. If  $\phi(\Omega_1(r), N - n_{\mathcal{C}}) < P$ , we add the corresponding vertex to the subgraph, which we now call  $\mathcal{C}'$ . If  $\phi(\Omega_1(r), N - n_{\mathcal{C}}) > P$ , one checks the second best vertex, the third best vertex, etc.. If there is finally a vertex, say the  $q$ -th best vertex, for which  $\phi(\Omega_q(r), N - n_{\mathcal{C}}) < P$ , one includes all  $q$  best vertices into subgraph  $\mathcal{C}$ , yielding subgraph  $\mathcal{C}'$ . At this point, no other vertex outside  $\mathcal{C}$  deserves to enter the community since all the external vertices are compatible with the statistics of the random configuration model. It may also happen that the inequality  $\phi < P$  above holds for no external vertex, in which case we add no vertices to  $\mathcal{C}$  and  $\mathcal{C}' = \mathcal{C}$ . Either way, we pass to the second stage with the subgraph  $\mathcal{C}'$ .

2. For each vertex  $i$  in  $\mathcal{C}'$  the variable  $r_i$  with respect to the set  $\mathcal{C}' \setminus \{i\}$  is estimated. We pick the “worst” vertex  $w$  of the cluster, i. e. the vertex with the highest value of  $r_i$ . To check for its significance we repeat step 1 for the subgraph  $\mathcal{C}' \setminus \{i\}$ . If  $w$  turns out to be significant, we keep it inside  $\mathcal{C}'$  and the analysis of the cluster is completed. Otherwise,  $w$  is moved out of  $\mathcal{C}'$  and one searches for the worst internal vertex of  $\mathcal{C}' \setminus \{w\}$ . At some point we end up with a cluster  $\mathcal{C}^*$ , whose internal vertices are all significant and the process stops.

The two-steps procedure is a way to “clean up”  $\mathcal{C}$ . A cluster is left unchanged only if all the external vertices are compatible with the null model and all the internal vertices are not. A few remarks are important here:

- There can be both *good* vertices outside  $\mathcal{C}$  and *bad* ones inside. It is important to perform the complete procedure described above, which guarantees that the final cluster is significant with respect to the present null model (see also Ref. [31]).
- The procedure is not deterministic, because of the stochastic component in the computation of the cumulative probability  $r$ . So one shall repeat all the steps several times. The cluster analysis may deliver a subgraph  $\mathcal{C}'$ , in general different from  $\mathcal{C}$ , or an empty subgraph. For each vertex  $i$  we compute the participation frequency  $f_i$ , defined as the ratio between the number of times  $i$  belongs to any non-empty  $\mathcal{C}'$  and the total number of iterations leading to non-empty subgraphs. In general, we consider the subgraph  $\mathcal{C}$  to be a significant cluster if the single cluster analysis yields a non-empty subgraph  $\mathcal{C}'$  in more than 50% iterations. The final “cleaned” cluster includes those vertices for which  $f_i > 0.5$ .
- In the worst-case scenario, the complexity of the cluster analysis scales with the number of vertices of  $\mathcal{C}$ , times the number of neighbors of  $\mathcal{C}$ , times the number of loops needed to have reliable values for the  $f_i$ 's. The situation can be considerably

improved by keeping track of the order of the external vertices at each step (using suitable data structures) and by computing the score only for some reasonably good vertices. For instance, one could pick just those vertices with  $r < 0.1$ . We numerically checked that changing this threshold does not affect the results, but leads to a faster algorithm.

### C. Network analysis

The previous procedure deals with a single cluster  $\mathcal{C}$ . It finds the external significant vertices and includes them into  $\mathcal{C}$ . It also prunes those internal vertices that are not statistically relevant. Now we extend this procedure by introducing an algorithm able to analyze the full network. In order to do so, we follow the method proposed by some of the authors in Ref. [23]. The starting point is a single vertex, taken at random, in the absence of any information. Let us suppose that we start from a random vertex  $i$  and that our first group is  $\mathcal{C} = \{i\}$ . The method proceeds as follows:

1.  $q$  vertices are added to  $\mathcal{C}$ , considering the most significant among the neighbors of the cluster. The number  $q$  is taken from a distribution, which in principle can be arbitrary. We choose a power law with exponent  $-3$ .
2. Perform the single cluster analysis.

We repeat the whole procedure starting from several vertices in order to explore different regions of the network. This yields a final set of clusters that may overlap. Such type of local optimization was originally implemented in the Local Fitness Method [23], to handle overlapping communities. The algorithm stops when it keeps finding *similar* modules over and over. Ideally one wishes to encounter the exact same clusters repeatedly. However, the stochastic element introduced when calculating the vertex score can lead vertices, whose score is close to the threshold, to change their group assignments from one realization to another. This can be a problem when we are trying to decide whether two groups in different instances correspond to the same cluster. As a practical rule, we say that two groups  $\mathcal{C}_1$  and  $\mathcal{C}_2$  are similar if  $|\mathcal{C}_1 \cup \mathcal{C}_2| / \min(|\mathcal{C}_1|, |\mathcal{C}_2|) > 0.5$ , in which case they deserve further attention. Indeed, it turns out that many of the clusters found are very similar or combinations of each other. This leads to a very important question: given a set of significant clusters, which ones should be kept?

Let us consider the problem of choosing between two clusters  $\mathcal{C}_1$  and  $\mathcal{C}_2$  and the union of the two,  $\mathcal{C}_3$ . A solution is to consider the subgraph  $\mathcal{G}_3$  of the vertices in  $\mathcal{C}_3$  and see if  $\mathcal{C}_1$  and  $\mathcal{C}_2$  are significant as modules of  $\mathcal{G}_3$ . Strictly speaking we consider  $\mathcal{C}'_1$  and  $\mathcal{C}'_2$  which are the cleaned up clusters within  $\mathcal{G}_3$  (i.e. with respect to subgraph  $\mathcal{G}_3$  only, neglecting the rest of the network). We discard  $\mathcal{C}_3$  if  $|\mathcal{C}'_1 \cup \mathcal{C}'_2| > P_2 \cdot |\mathcal{C}_3|$ , where we set  $P_2 = 0.7$ .

Otherwise we discard  $\mathcal{C}_1$  and  $\mathcal{C}_2$  and we keep the union  $\mathcal{C}_3$ . Instead, if we have to decide among a set of  $k$  clusters and their union, the condition to prefer the submodules is  $|\cup_i \mathcal{C}'_i| > P_2 \cdot |\mathcal{C}_u|$ .

In general, we check if each cluster has significant submodules, by looking for modules in the subgraph given by the cluster and using the condition above to decide which ones to take. This leads to a set of significant minimal clusters, where minimal means that they have no significant internal cluster structure, according to the condition above. We also need to check whether unions of such minimal clusters do have internal cluster structure, according to our rule, to decide whether the clusters have to be kept separated or merged. After doing this, we still end up with many *similar* modules. Given a pair of similar modules (in the sense defined above), we first check if their union has significant cluster structure: if it does not, we merge the two clusters, otherwise we systematically prefer the bigger one (if they are equal-sized, we pick the cluster with smaller score).

After the completion of this procedure, the output is a cover of the network. To reduce the stochasticity introduced by the bootstrap, the procedure is repeated in order to obtain several covers. All clusters of the covers are analyzed as described above to select among them the ones which will appear in the final output.

### D. OSLOM

We have described the cleaning of a single cluster and how the full network is analyzed. In the following, all the ingredients are assembled together to form the algorithm that we call OSLOM (Order Statistics Local Optimization Method).

A flux diagram summarizing how it works can be seen in Fig. 4. OSLOM consists of three phases:

- First, it looks for significant clusters, until convergence;
- Second, it analyzes the resulting set of clusters, trying to detect their internal structure or possible unions thereof;
- Third, it detects the hierarchical structure of the clusters.

To speed up the method, one can start from a given partition/cover delivered by another (fast) algorithm or from *a priori* information. In those cases, the first step will be to clean up the given clusters.

Once the set of minimal significant clusters has been found, the analysis of the hierarchies consists of the following steps. We construct a new network formed by clusters, where each cluster is turned into a supervertex and there are edges between supervertices if the representative clusters are linked to each other. The resulting superedges are weighted by the number of edges between

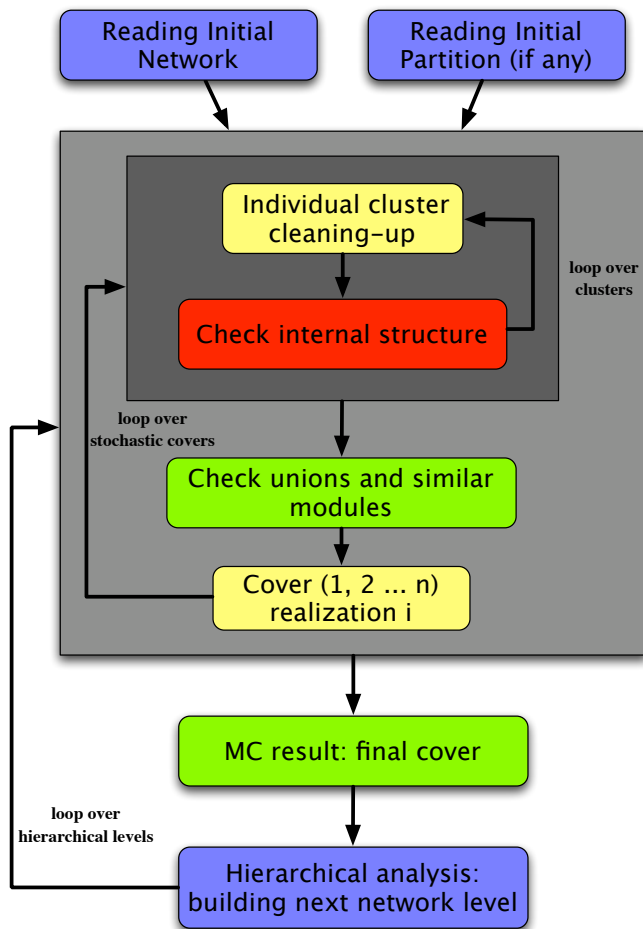


Figure 4: Flux diagram of OSLOM. The levels of grey of the squares represent different loop levels. One can provide an initial partition/cover as input, from which the algorithm starts operating, or no input, in which case the algorithm will build the clusters about individual vertices, chosen at random. OSLOM performs first a cleaning procedure of the clusters, followed by a check of their internal structure and by a decision on possible cluster unions. This is repeated with different choices of random numbers in order to obtain better statistics and a more reliable information. The final step is to generate a super-network for the next level of the hierarchical analysis.

the initial clusters. There is the problem of properly assigning edges between clusters, if the edges are incident on overlapping vertices. Suppose to have an edge whose endvertices  $i$  and  $j$  belong to  $\nu_i$  and  $\nu_j$  clusters, respectively. This edge lies simultaneously between any pair of clusters  $\mathcal{C}_i$  and  $\mathcal{C}_j$ , with  $\mathcal{C}_i$  including  $i$  and  $\mathcal{C}_j$  including  $j$ . The contribution of the edge to the superedge between  $\mathcal{C}_i$  and  $\mathcal{C}_j$  equals  $1/(\nu_i \cdot \nu_j)$ . The resulting non-integer weights may lead to non-integer values for the weight of superedges, whereas we need integer values in order to use Eq. 1. For this reason, the weight of each superedge is rounded to the nearest integer value. We stress that the weight we deal with here indicates just how to “split”

edges, it is not related to the weight that edges may carry. If the original network is weighted, the rescaled weight of an edge is  $w/(\nu_i \cdot \nu_j)$ ,  $w$  being the weight of the edge in the network. Once the supernetwork has been built, one applies the method again, obtaining the second hierarchical level. The latter is turned again into a supernetwork, as we explained above, and so on, until the method produces no clusters. In this way OSLOM recovers the hierarchical community structure of the original graph.

We will describe next the main features of OSLOM, and what it adds to the state of the art in community detection.

### 1. Significant clusters

The main characteristic of OSLOM is that it is based on a fitness measure, the score, that is tightly related to the significance of the clusters in the configuration model. In fact, the single cluster analysis is designed to optimize the cluster significance as defined in Ref. [31]. Therefore the output of OSLOM consists of clusters that are unlikely to be found in an equivalent random graph with the same degree sequence. The tolerance  $P$ , fixed initially, determines whether such clusters are “unexpectedly unlikely”, and therefore significant, or not. So, if the method is fed with a random graph, the output will include very few clusters or even none at all.

### 2. Homeless vertices

The vertices in a random network will be deemed as homeless. Homeless vertices are those that are not assigned to any cluster. This is a very important feature that OSLOM includes. The presence of random noise or non-significant vertices is an issue that may occur in many real systems. However, very few clustering techniques take into account this possibility. In OSLOM, it comes as a natural output. We will quantitatively analyze this feature when we test the method on benchmark graphs.

### 3. Overlapping communities

A natural output of OSLOM is the possibility for clusters to overlap. Since each cluster is “cleaned” independently of the others, a fraction of its vertices may belong also to other clusters, eventually. We will show the efficiency of OSLOM in unveiling overlapping vertices in suitably designed benchmarks.

### 4. Cluster hierarchy

Another relevant feature of OSLOM is the analysis of the hierarchical structure of the clusters. As mentioned

above, the third phase of our method includes a procedure to take care of this issue. The results are very good on hierarchical benchmarks.

OSLOM generally finds different depths in different hierarchical branches. In fact, when the algorithm is applied not all vertices are grouped, as some of them are homeless. The coexistence of homeless vertices with proper clusters yields a hierarchical structure with branches of different depths.

### 5. Weighted networks

OSLOM can be generalized to weighted graphs as well. We assume that the contributions to the probability of having a connection between two vertices  $i$  and  $j$  with a certain weight  $w_{ij}$ , given the vertex degrees  $k_i$  and  $k_j$  and their strengths,  $s_i$  and  $s_j$ , is separable in two different terms in the configuration model: one for the topology and another for the weight [38]. The strength of a vertex is defined as the sum of the weights of all the edges incident on it. We approximate the weight contribution by

$$p(w_{ij} > x | k_i, k_j, s_i, s_j) = \exp(-x / \langle w_{ij} \rangle), \quad (5)$$

where  $\langle w_{ij} \rangle = 2\langle w_i \rangle \langle w_j \rangle / (\langle w_i \rangle + \langle w_j \rangle)$  is the harmonic mean of the average weights of vertices  $i$  and  $j$ , defined as  $\langle w_i \rangle = s_i / k_i$  and  $\langle w_j \rangle = s_j / k_j$ , respectively. The idea behind this expression is that the weight of an edge of the null model should be proportional to the average weight of its endvertices. We proposed the harmonic average because it is more sensitive to the small values of  $\langle w \rangle$ .

We use this distribution to define a new variable  $r_w$ , accounting for the probability of having a certain weight on a given edge with the strengths of the vertices and the general weight distribution known. We combine this variable  $r_w$  with its topological counterpart,  $r_t$ , obtaining a new variable  $r_{wt}$ . This is a non-trivial task since both probabilities are defined on a different set of elements (see the Supporting Information S1). For  $r_{wt}$  we can estimate, as before, the order statistic distributions and we proceed just as we do for unweighted graphs.

### 6. Directed graphs

OSLOM can be easily generalized to handle directed graphs. For that, we need to define two uniformly distributed random variables  $r_{out}$  and  $r_{in}$ . The former is based on the probability that vertex  $i$  has outgoing edges ending on vertices of the given subgraph  $\mathcal{C}$ , the latter is based on the probability that  $i$  has incoming edges originating from vertices of  $\mathcal{C}$ . These two probabilities are computed through analogous formulas as in Eq. 1 or numerical approximations to it. The final score of vertex  $i$  is given by the product  $r_{in} \cdot r_{out}$ . We are able to calculate the distribution of this product and therefore to

estimate its order statistics (just as for the weighted case, see Section 1.1. of Supporting Information S1). The rest of the clustering method proceeds as explained above. If graphs have edges with both directions and weights, we have four variables for each vertex:  $r_{in}$ ,  $r_{out}$  and the corresponding versions for the weights. The final score is given again by the product of these four variables.

### 7. Dynamical networks

Time-stamped networked datasets are usually divided into snapshots, condensing the relational information between vertices within different time windows. Snapshots are typically analyzed separately, whereas it would be more informative to combine the information from different time slices. For instance, consider two snapshots  $\mathcal{G}_t$  and  $\mathcal{G}_{t+\Delta t}$  at times  $t$  and  $t + \Delta t$ , respectively. A simple idea is to find the partition/cover of the network at time  $t$ , by applying the method to the corresponding snapshot, and to use the result as an input for the application of the method to the network at time  $t + \Delta t$ . In this way one can see how the community structure at time  $t$  “evolves” to that at time  $t + \Delta t$ . This is a rather general approach, it can be adopted for other algorithms for community detection, like greedy optimization techniques. OSLOM has the useful property that it can start from any initial partition/cover, which can be given as input. In this way the clusters found in  $\mathcal{G}_t$  can be used as initial condition for the analysis of  $\mathcal{G}_{t+\Delta t}$ . With this approach, the new partition/cover is closer to that in  $\mathcal{G}_t$  and we are able to track the groups’ evolution. Naturally, if the two snapshots are very different from each other (because they refer to times between which the system has changed considerably, for instance), OSLOM produces a partition/cover in  $\mathcal{G}_{t+\Delta t}$  that is uncorrelated with that of  $\mathcal{G}_t$ .

### 8. Complexity

The complexity of OSLOM cannot be estimated exactly, as it depends on the specific features of the community structure at study. Therefore we carried out a numerical study of the complexity, whose results are shown in Fig. 5.

We apply the method on the LFR benchmark [41], that we have used extensively to test the performance of OSLOM. We have used both the standard version of the algorithm and a fast implementation, in which the algorithm acts on the partition delivered by a quick method. For each version we have considered undirected and unweighted LFR benchmark graphs with two different levels of mixtures between the clusters ( $\mu = 0.1$  and  $\mu = 0.6$ , corresponding to well separated and well mixed clusters). The other parameters needed to build the LFR benchmark graphs are the same as for the graphs used in Fig. 6. The diagram of Fig. 5 shows the execution time (in

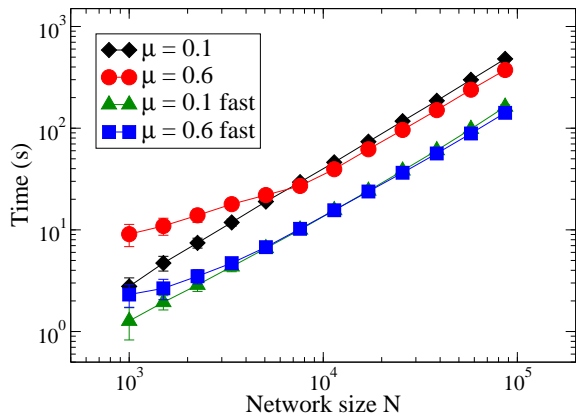


Figure 5: Complexity of OSLOM. The diagram shows how the execution time of two different implementations of the algorithm scales with the network size (expressed by the number of vertices), for LFR benchmark graphs.

seconds) as a function of the number  $N$  of vertices of the graphs. The processes were run on a workstation HP Z800. The time scales as a power law of  $N$  with good approximation, if the graphs are not too small. The behavior seems to depend neither on how mixed communities are, nor on the particular implementation of the algorithm (there seems to be just a factor between the corresponding curves). Power law fits of the large- $N$  portion of the curves yield an exponent 1.1(1), which implies that the complexity is essentially linear in this case.

### III. RESULTS

#### A. Artificial networks

In this section we test OSLOM against artificial benchmarks, comparing its performance with those of the best algorithms currently available. We mostly adopted the LFR benchmark [41, 42], a class of graphs with planted community structure and heterogeneous distributions of vertex degree and community size. Tests on the well known Girvan-Newman (GN) benchmark [8] are shown in the Supporting Information S1. In this section we present tests on undirected and unweighted networks, with and without hierarchical structure and overlapping communities. We also show how OSLOM handles the presence of randomness in the graph structure. Tests on weighted networks and on directed networks can be found in the Supporting Information S1.

In the following sections, for each network, we compose the results of 10 iterations for the network analysis for the first hierarchical level and the results of 50 iterations for higher levels, if any. The single cluster analysis was

repeated 100 times for each cluster.

#### 1. LFR benchmark

The LFR benchmark [41, 42], like the GN benchmark, is a particular case of the *planted  $\ell$ -partition model* [43], which is the simplest possible model of networks with communities. The planted  $\ell$ -partition model is a class of graphs whose vertices are divided into  $\ell$  equal-sized groups, such that the probability that two vertices of the same group are linked is  $p$ , while the probability that two vertices of different groups are linked is  $q$ , with  $p > q$ . The planted  $\ell$ -partition model is too simple to describe real networks. Vertices have essentially the same degree and communities have the same size, at odds with empirical analysis showing that both features typically are broadly distributed [19, 44–48]. Therefore we have recently proposed a generalization of the model, the LFR benchmark, by introducing power-law distributions for the vertex degree and the community size, with exponents  $\tau_1$  and  $\tau_2$ , respectively [41]. The LFR benchmark poses a far harder challenge to algorithms than the benchmark by Girvan and Newman, which is regularly used in the literature, and is more suitable to spot their limits. We are of course aware that the communities of the model are still too simple to match the communities of real networks. Other features should be introduced, to tailor the model graphs onto the real graphs. This is certainly doable, and could be specialized to the particular domain of applicability one is interested in. Still, the clusters of the LFR benchmark are a much better proxy of real communities than the clusters of other benchmark graphs.

Vertices of the LFR benchmark have a fixed degree (in this case taken from the given power law distribution), so the two parameters  $p$  and  $q$  of the planted  $\ell$ -partition model are not independent and we choose as independent variable the *mixing parameter*  $\mu$ , which is the ratio of the number of external neighbors of a vertex by the total degree of the vertex. Small values of  $\mu$  indicate well separated clusters, whereas for higher and higher values communities become more and more mixed to each other.

As a term of comparison we used Infomap [49], which has proved to be very accurate on artificial benchmark graphs [50]. Fig. 6 shows the comparative performance of OSLOM and Infomap on the LFR benchmark, with undirected and unweighted edges and non-overlapping clusters. As a measure of similarity between the planted partition and that recovered by the algorithm we adopted the Normalized Mutual Information (NMI) [51], in the extended version proposed in Ref. [23], which enables one to compare both partitions and covers. We used this definition also for hard planted partitions, since modules found by OSLOM may be overlapping. In all tests on artificial graphs each point is always an average over 100 realizations.

The plots correspond to two network sizes,  $N = 1000$



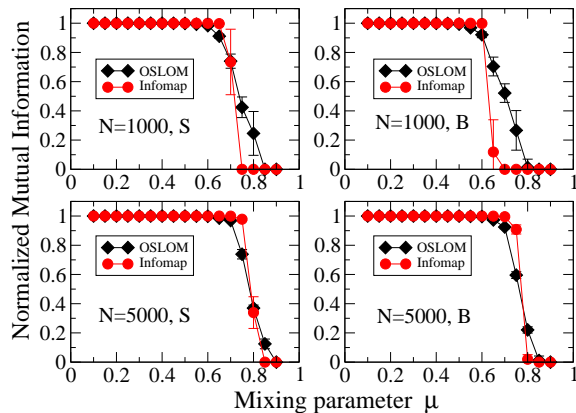


Figure 6: Tests on undirected and unweighted LFR benchmark graphs without overlapping communities. The parameters of the graphs are: average degree  $\langle k \rangle = 20$ , maximum degree  $k_{max} = 50$ , exponents of the power law distributions are  $\tau_1 = 2$  for degree and  $\tau_2 = 1$  for community size, S and B mean that community sizes are in the range  $[10, 50]$  (“small”) and  $[20, 100]$  (“big”), respectively. We considered two network sizes:  $N = 1000$  (top) and  $N = 5000$  (bottom). The two curves refer to OSLOM (diamonds) and Infomap (circles).

and  $N = 5000$ , and two ranges of community size,  $[10, 50]$  (“small”) and  $[20, 100]$  (“big”), that we indicate with the letters S and B, respectively. In this way we can check how much the performance of the algorithm is affected by the network size and the average size of the communities. The other network parameters are given in the caption. From the plots we conclude that OSLOM and Infomap have a basically equivalent performance.

It is important to test the performance of the algorithms on large graphs as well, given the increasing availability of large networked datasets. The question is if and how their performance is affected by the network size. Fig. 7 shows that both OSLOM and Infomap are effective at finding communities on large LFR graphs. We remark that the inferior accuracy of OSLOM when communities are better defined comes from the fact that the method occasionally finds homeless vertices, i.e. vertices that are not significantly linked to any cluster. These are vertices that happen not to have a significant excess of neighbors within their community with respect to the number of neighbors in the other communities, despite the fact that the average number of internal neighbors is high. This happens because of fluctuations, and the method judges such vertices as not belonging to any group, which makes sense. This issue of the homeless vertices is a general feature of OSLOM. One should not judge it negatively, though. If a vertex  $i$  happens to have a number of external neighbors which is appreciably higher than the expected external degree of the vertex  $\mu k_i$ , the condition  $p > q$  of the planted  $\ell$ -partition model does not hold, so

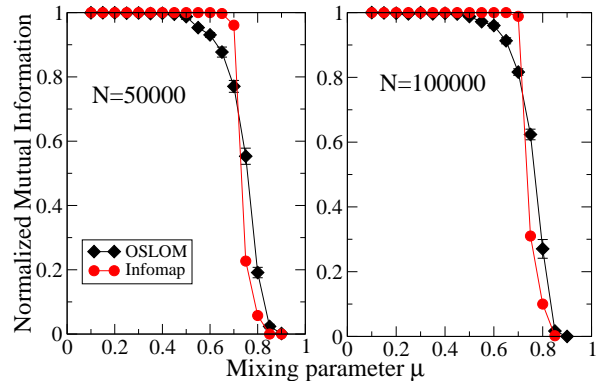


Figure 7: Tests on large undirected and unweighted LFR benchmark graphs without overlapping communities. The network sizes are  $N = 50000$  (left) and  $N = 100000$  (right), the maximum degree  $k_{max} = 200$  and the community size ranges from 20 to 1000. The other parameters are the same as those used for the graphs of Fig. 6. The two curves refer to OSLOM (diamonds) and Infomap (circles).

in principle the vertex should not be put in its original community. The confusion derives from the fact that the condition  $p > q$  holds *on average*.

## 2. LFR benchmark with overlapping communities

The LFR benchmark also accounts for overlapping communities, by assigning to each vertex an equal number of neighbors in different clusters [42]. To simplify things, we assume that each vertex belongs to the same number of communities. We cannot use Infomap for the comparison, as it delivers “hard” partitions, without overlaps between clusters. So we used two recent methods, that have a good performance on LFR graphs with overlapping communities: COPRA [52], based on label propagation [53], and MOSES [54], based on stochastic block modeling [55]. COPRA and MOSES are more efficient to detect overlapping communities in LFR benchmark graphs than the popular Clique Percolation Method (CPM) [19], which is the reason why we do not use the CPM here. In Fig. 8 we show how the performance of each method decays with the fraction of overlapping vertices, for different choices of the mixing parameter and for the small (S) and big (B) communities defined above. Since in social networks there may be many vertices belonging to several groups, we also considered the extreme situation of graphs consisting entirely of overlapping vertices. In this case, by increasing the number of memberships of the vertices communities become more fuzzy and it gets harder and harder for any method to

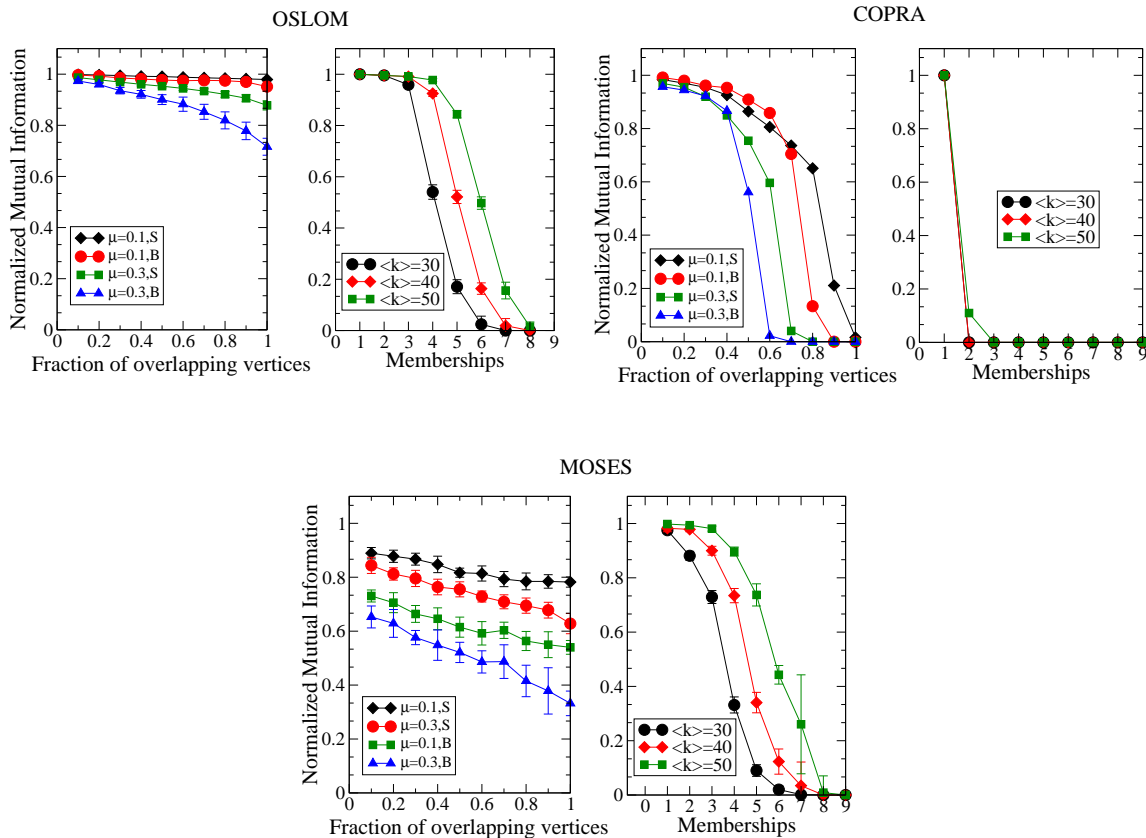


Figure 8: Test on undirected and unweighted LFR benchmark with overlapping communities. The parameters are:  $N = 1000$ ,  $\langle k \rangle = 20$ ,  $k_{max} = 50$ ,  $\tau_1 = 2$ ,  $\tau_2 = 1$ . S and B indicate the usual ranges of community sizes we use:  $[10, 50]$  and  $[20, 100]$ , respectively. We tested OSLOM against two recent methods to find covers in graphs: COPRA [52] and MOSES [54]. The left panel displays the normalized mutual information (NMI) between the planted cover and the one recovered by the algorithm, as a function of the fraction of overlapping vertices. Each overlapping vertex is shared between two clusters. The four curves correspond to different values of the mixing parameter  $\mu$  (0.1 and 0.3) and to the community size ranges S and B. The right panel shows a test on graphs whose vertices are all shared between clusters. Each vertex is member of the same number of clusters. The plot shows the NMI as a function of the number of memberships of the vertices. Each curve corresponds to a given value of the average degree  $\langle k \rangle$ . The graph parameters are  $N = 2000$ ,  $k_{max} = 60$ ,  $\mu = 0.2$ ,  $\tau_1 = 2$ ,  $\tau_2 = 1$ . Community sizes are in the range  $[20, 50]$ .

correctly identify the modules. From Fig. 8 we deduce that OSLOM significantly outperforms COPRA in both tests and MOSES in the test with overlapping and non-overlapping vertices, while the performances of OSLOM and MOSES are quite close when all vertices are overlapping.

### 3. Hierarchical LFR benchmark

OSLOM is capable to handle hierarchical community structure as well. To test its performance we have designed an algorithm that produces a version of the LFR benchmark with hierarchy. To keep things simple, we consider a two-level hierarchical structure (Fig. 9). The idea is to use the wiring procedure of the original algo-

rithm twice, first for the micro-communities and then for the macro-communities. In order to do so, we need two mixing parameters:  $\mu_1$ , the fraction of neighbors of each vertex belonging to different macro-communities;  $\mu_2$ , the fraction of neighbors of each vertex belonging to the same macro-community but to different micro-communities. The question is whether the algorithm is able to recover both planted partitions of the benchmark, which we call *Fine* (micro-communities) and *Coarse* (macro-communities). The partitions found by the algorithm can be one, two or more, we call them partition 1, 2, 3, ... In the test, whose results are illustrated in Fig. 10, we compare the Fine partition with partition 1 (Fine 1), the Coarse partition with partition 2 (Coarse 2), and the Coarse partition with partition 1 (Coarse 1). We compare OSLOM with a recent extension of Infomap to networks

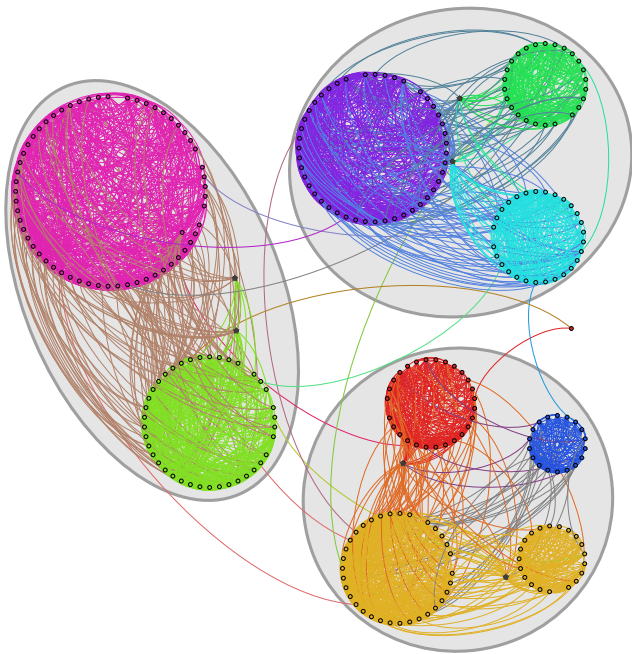


Figure 9: A realization of the hierarchical LFR benchmark with two levels. Stars indicate overlapping vertices.

with hierarchical community structure [56]. In the plots we show how the similarity of the three pairs of partitions mentioned above varies by increasing  $\mu_2$  but keeping  $\mu_1$  constant (we picked the values  $\mu_1 = 0, 0.1, 0.2, 0.3$ ). For a better comparison of the panels we put on the x-axis the sum  $\mu_1 + \mu_2$ , representing the fraction of neighbors of a vertex not belonging to its micro-community. We find that, when  $\mu_2$  increases, the Fine partition becomes difficult to resolve and, for  $\mu_1 + \mu_2 \gtrsim 0.7$ , it cannot be found anymore and both algorithms can only find the Coarse partition. Instead, for smaller value of  $\mu_2$ , the algorithms can recover both levels. OSLOM performs better than Infomap if  $\mu_1$  is not too small.

#### 4. Random graphs and noise

We check whether OSLOM is also able to recognize the *absence*, and not simply the presence, of community structure. In random graphs vertices are connected to each other at random, modulo some basic constraints like, e. g., keeping some prescribed degree distribution or sequence. In this way, there are by definition no groups of vertices that preferentially link to each other, so there are no communities. There may be subgraphs with an internal edge density higher than the average edge density of the whole network, but they originate from stochastic fluctuations (noise). A good community finding algorithm should be able to recognize that such subgraphs are false positives, and discard them. Here we want to see if OSLOM distinguishes “order” from “noise”. For this

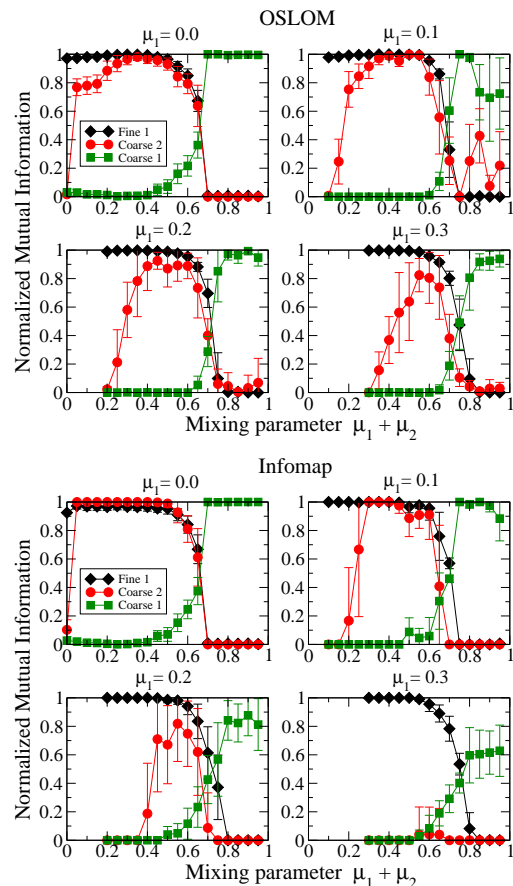


Figure 10: Test on hierarchical LFR benchmark graphs (unweighted, undirected and without overlapping clusters). We compare three pairs of partitions: the lowest hierarchical partition found by the algorithm (indicated by 1) with the set of micro-communities of the benchmark (Fine); the lowest hierarchical partition found by the algorithm with the set of macro-communities of the benchmark (Coarse); the second lowest hierarchical partition found by the algorithm (indicated by 2) with the set of macro-communities of the benchmark. The corresponding similarities are plotted as a function of  $\mu_1 + \mu_2$ , for fixed  $\mu_1$ . There are 10000 vertices, the average degree  $\langle k \rangle = 20$ , the maximum degree  $k_{max} = 100$ , the size of the macro-communities lies between 400 and 4000 vertices, the size of the micro-communities lies between 10 and 100 vertices. The exponents of the degree and community size distributions are  $\tau_1 = 2$  and  $\tau_2 = 1$ .

purpose, we carried out two tests. In Fig. 11 we applied OSLOM and Infomap to Erdős-Rényi random graphs [57] and scale-free networks [58]. The goal is to see whether the algorithms recognize that there are no actual communities. Good answers are the partition with as many communities as vertices, or the partition with all vertices in the same community. Let us call  $\mathcal{P}$  the partition found by the algorithm at hand. Clusters in  $\mathcal{P}$  containing at least two vertices and smaller than the whole network indicate that the method has been fooled. The fraction of graph vertices belonging to those clusters is a measure

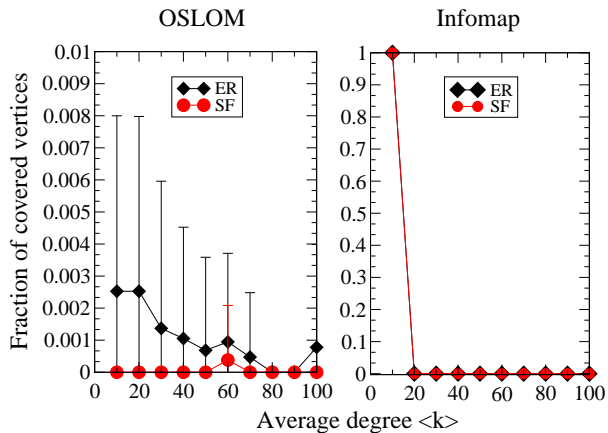


Figure 11: Test on random graphs. We plot the fraction of vertices belonging to non-trivial clusters (i.e. to clusters with more than one and less than  $N$  vertices, where  $N$  is as usual the size of the graph), as a function of the average degree of the graph. The curves correspond to Erdős-Rényi graphs (diamonds) and scale-free networks (circles). All graphs have  $N = 1000$  vertices. The only parameter needed to build Erdős-Rényi graphs is the probability that a pair of vertices is connected, which is determined by the average degree  $\langle k \rangle$ . The scale-free networks were built with the configuration model [39], starting from a fixed degree sequence for the vertices obeying the predefined power law distribution. The parameters of the distribution are: degree exponent  $\gamma = 2$ , maximum degree  $k_{max} = 200$ .

of reliability: the lower this number, the better the algorithm. In Fig. 11 we show this variable as a function of the average degree  $\langle k \rangle$  of the random graphs we considered. For OSLOM it remains very low for all values of  $\langle k \rangle$ . This is not surprising, since OSLOM estimates the statistical significance of clusters, and is therefore ideal to detect stochastic fluctuations. Infomap instead finds many non-trivial clusters when  $\langle k \rangle$  is low, whereas it correctly recognizes the absence of community structure if  $\langle k \rangle$  increases.

The second test deals with graphs consisting of an *ordered* part, with well-defined clusters, and a *noisy* part, consisting of vertices randomly attached to the rest of the network. The ordered part is an LFR benchmark graph with 1000 vertices and represents the starting configuration of our system. The noisy vertices (up to 2000 in number) are successively added in sequence, and a newly added vertex is linked to the other ones via preferential attachment [58]. The initial degree of the noisy vertices is drawn from a power law distribution with  $k_{max} = 100$  and exponent 3. We measure two things, as a function of the number of noisy vertices: the similarity between the set of noisy vertices and the set of homeless vertices found by OSLOM, which is expressed by the Jaccard Index [59] (Fig. 12, left); the similarity between the planted parti-

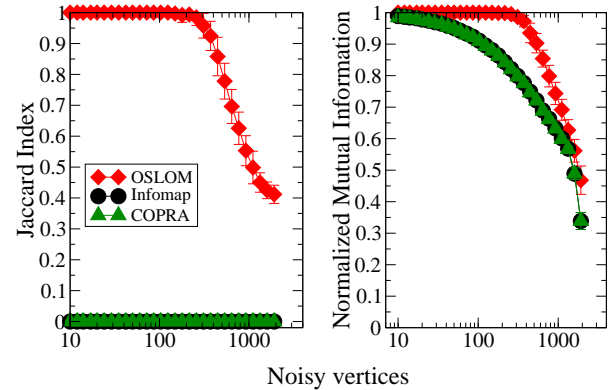


Figure 12: Test on graphs including communities and noise. The communities are those of an LFR benchmark graph (undirected, unweighted and without overlapping clusters), with  $N = 1000$ ,  $\langle k \rangle = 20$ ,  $k_{max} = 50$ ,  $\mu = 0.2$ . The cluster size ranges from 10 to 50 vertices. The noise comes by adding vertices which are randomly linked to the existing vertices, via preferential attachment. The test consists in checking whether the community finding algorithm at study (here OSLOM, Infomap and COPRA) is able to find the communities of the planted partition of the LFR benchmark and to recognize as homeless the other vertices.

tion of the ordered part of the graph and the subset of the partition found by OSLOM including (only) the vertices of the ordered part, which is expressed by the normalized mutual information (Fig. 12, right). We compare OSLOM with Infomap and COPRA [52]. We find that OSLOM correctly separates the clusters and the noise up to a number of about 300 noisy vertices, which represent almost a third of the whole network. Infomap and COPRA, instead, do not recognize the noisy vertices, no matter how small their number is. Also, they tend to mix noisy vertices with the clusters of the planted partition of the ordered part, as shown by the fact that the partition they recover never exactly match the planted partition, not even when just a few noisy vertices are present. These results are actually understandable in the case of Infomap, which is based on the minimization of the code length required to describe random walks taking place on the graph: singletons (clusters consisting of single vertices) are generally not admitted because they increase the amount of information required to map the process, due to the high number of transitions of the walker from the singletons to the rest of the graph and back.

## B. Real networks

In this section we discuss the application of OSLOM to networks from the real world. In Table 1 we list the net-

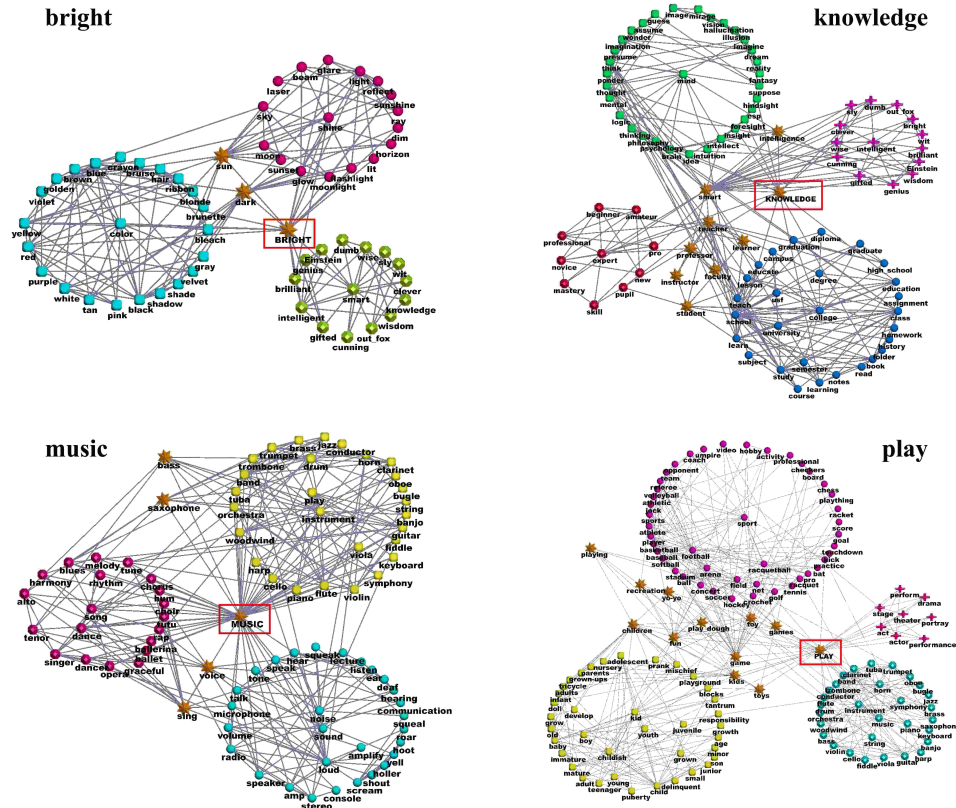


Figure 13: Application of OSLOM to real networks: the word association network. Stars indicate overlapping vertices.

works considered in our analysis, along with some basic statistics obtained from the detection of their community structure with OSLOM.

We analyzed different types of systems: social, information, biological and infrastructural networks. Here we discuss only some of them, the rest of the analysis can be found in Appendix D.

### 1. The word association network

This network is built on the University of South Florida Free Association Norms [60]. Here the presence of an edge between words  $A$  and  $B$  indicates that some people associate  $B$  to the word  $A$ . This network is considered a paradigmatic example of graph with overlapping communities [19], since several words may have various meanings and belong to different groups of words. In Fig. 13 we see a few subgraphs of the word association network, revolving around four keywords: *bright*, *knowledge*, *music* and *play*. We see that the keywords are shared among several clusters, which are semantically highly homogeneous. For instance, *bright* belongs to three groups, centered on the words *color*, *shine* and *smart*, respectively, which makes sense. In the same subgraph, the words *sun* and *dark* are also overlapping vertices, belonging to the

groups of *color* and *shine*, as one might expect. In the subgraph centered on *knowledge*, one distinguishes the groups referring to the words *mind*, *intelligent*, *expert* and *college/university*. Here there are many overlapping vertices, like the word *intelligence*, shared between the groups of *mind* and *intelligent*, and a bunch of terms indicating (mostly) professional status within schools and/or universities, like *student*, *professor*, *teacher*, etc., which lie between the groups of *expert* and *college/university*. In the third subgraph, the word *music* is shared by the groups of *instrument*, *song/dance* and *noise/sound*: other overlapping vertices are the words *sing* and *voice*, lying between *song/dance* and *noise/sound*, and the words *bass* and *saxophone*, belonging to the groups of *song/dance* and *instrument*. Finally, the word *play* sits between the communities of *sport*, *music* and *youth/kid*; other overlapping vertices in this subgraph include *game*, *children*, *toy*, etc..

### 2. UK commuting

This is the network of flows of commuters between areas of the United Kingdom, and therefore it has a clearly geographic character. It is composed of 10 608 vertices, each representing a ward, i. e. a geographi-

Network	$N$	$E$	$\langle k \rangle$	$N_c$	$\langle s \rangle$	$\langle m \rangle$	$f_h$
Zachary's club	34	78	4.59	2	17.0	1.03	0.0294
Dolphins	62	159	5.13	2	32.5	1.08	0.0322
Football	115	613	10.7	11	10.0	1.00	0.0434
UK commuting	10 608	1 220 337	230.07	248	45.43	1.06	0.00386
<i>C. elegans</i>	453	2 025	8.94	25	17.04	1.22	0.229
Word association	7 207	31 784	8.82	261	22.48	1.35	0.395
Live Journal	4 846 609	42 851 237	17.6	407 451	10.01	1.19	0.294
www. uk	18 484 117	292 244 462	15.81	590 257	28.08	1.02	0.125
US airports 2009 (jan)	448	7 659	34.19	11	33.81	1.28	0.352
US airports 2009 (mar)	456	8 491	37.24	6	67.83	1.22	0.272
US airports 2009 (jun)	453	8 480	37.42	9	45.33	1.28	0.315
US airports 2009 (sep)	452	7 870	34.81	9	41.55	1.26	0.347

Table I: Basic statistics of the real networks we analyzed, including the main features of their community structure, detected by OSLOM. From left to right, we list the number of vertices  $N$  and edges  $E$ , the average degree  $\langle k \rangle$ , the number of clusters  $N_c$ , the average cluster size  $\langle s \rangle$ , the average number of memberships per vertex  $\langle m \rangle$  and the fraction  $f_h$  of vertices not assigned to any cluster (homeless vertices). The values related to the community structure refer to the lowest hierarchical level.

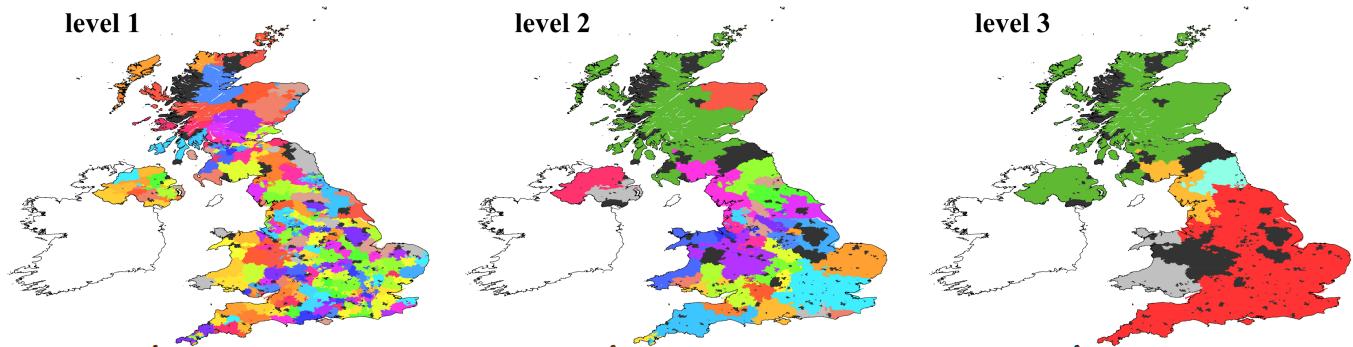


Figure 14: Application of OSLOM to real networks: flows of commuters in the UK. Black points indicate overlapping vertices.

cal division used in the UK census for statistical purposes. The whole territory of the United Kingdom is divided into wards. Each edge corresponds to a flow of commuters between the ward of origin and that of destination, with a weight accounting for the number of commuters per day. The data were collected during the 2001 UK census, when the ward of residence and the ward of work/study was registered for a sizeable part of the British population. The database can be accessed online at the site of the Office for National Statistics <http://www.ons.gov.uk/census>. OSLOM finds three hierarchical levels (Fig. 14). The clusters of the second level delimit geographical areas typically centered about one major town. In the highest level the areas of England, Wales, Scotland and Northern Ireland are clearly recognizable. Interestingly, Northern Ireland and Scotland are parts of the same community, due to the large flow of commuters between the two regions, despite the geographical separation. Black points represent overlapping vertices.

### 3. *LiveJournal and UK Web*

We also applied OSLOM to two large networks. The first is a network of friendship relationships between users of the on-line community *LiveJournal* ([www.livejournal.com](http://www.livejournal.com)), and was downloaded from the Stanford Large Network Dataset Collection (<http://snap.stanford.edu/data/>). The second is a crawl of the Web graph carried out by the Stanford WebBase Project (<http://dbpubs.stanford.edu:8091/~testbed/doc2/WebBase/>), within the UK domain (.uk). We remind that the Web graph is a directed graph whose vertices are Web pages, while the edges are the hyperlinks that enable one to surf from one page to another. These two systems are too large for OSLOM, due to the huge variety of possible cluster sizes to explore. Therefore we applied a two-step method: in the first step, we derived an initial partition  $\mathcal{P}^*$  with the Louvain method [61], which is able to handle large networked datasets; in the second step, we apply OSLOM to refine the clusters of  $\mathcal{P}^*$ . In principle, this

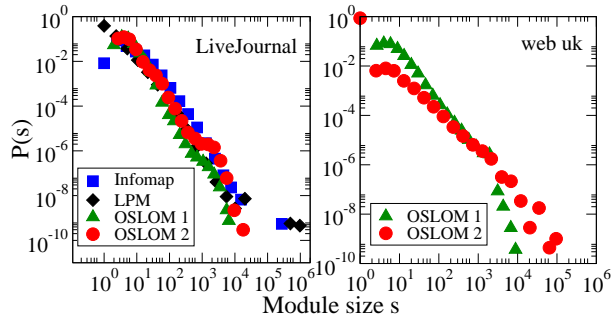


Figure 15: Application of OSLOM to real networks: friendships of *LiveJournal* users (left) and sample of the .uk domain of the Web graph (right). We show the distribution of cluster sizes obtained by OSLOM for the first two hierarchical levels (OSLOM 1 and OSLOM 2). For *LiveJournal* we can compare the distributions with those found with Infomap [49] and the Label Propagation Method (LPM) by Leung et al. [62].

procedure should yield the same partitions/covers as applying OSLOM directly, if one repeated OSLOM’s cluster search many times. But this would make the calculations too lengthy, so, in order to complete the analysis within a reasonable time, it is necessary to keep the number of iterations low. In this way there is the big advantage of drastically reducing the computational complexity, which makes large systems tractable, even if results would be more accurate if one could apply OSLOM from scratch. Clearly, since different iterations are independent processes, one could sensibly increase the statistics by distributing the iterations among different processors, if available.

In Fig. 15 we present the distribution of cluster sizes of the first two hierarchical levels found by OSLOM. The results are obtained by performing a single iteration on a workstation HP Z800. For the Web graph, which is the larger system, with nearly 20 million vertices and 300 million edges (see Table 1), the analysis was completed in about 40 hours. For the social network of *LiveJournal* we can compare the results with the corresponding distributions found by Infomap and the Label Propagation Method (LPM) proposed by Leung et al. [62], which were computed in a recent analysis [48]. In that work the original Infomap was used, so neither Infomap nor the LPM could detect hierarchical community structure and there is just one cluster size distribution, corresponding to the single partition recovered. The distributions are broad and quite similar across different methods. Interestingly, the two hierarchical levels of *LiveJournal* (OSLOM 1 and OSLOM 2) are not too different, indicating a sort of self-

similarity of the community structure. For the Web the two levels are more dissimilar and the distributions have a clear power law decay (with different exponents) up to a cutoff, which is approximately the same for both curves ( $\sim 2000$  vertices).

#### 4. Dynamic datasets: the US air transportation network

For the last application, we used a time-stamped dataset, the US air transportation network. The data can be downloaded from the Bureau of Transportation Statistics (US government) (<http://www.bts.gov>). Vertices are airports in the USA and edges are weighted by the number of passengers transported along the corresponding routes. In Fig. 16 we show the geographical location of the airports and their communities, indicated by the symbols, for three snapshots, corresponding to the traffic in March, June and September 2009, respectively. We remind that for dynamical datasets we usually take the partition/cover  $\mathcal{P}(t)$  of the system at time  $t$ , and we use it as initial partition/cover for the topology of the system at time  $t + \Delta t$ , which is then refined by OSLOM, in order to “adapt”  $\mathcal{P}(t)$  to the current structure. This is done to exploit the information of more snapshots at the same time. Since the three maps of Fig. 16 are mostly illustrative, communities were derived by applying directly OSLOM to the corresponding snapshots, for simplicity. The diagram indicates the similarity between networks and their corresponding partitions/covers in different snapshots. Each snapshot represents the whole traffic of one trimester, which corresponds to a season, while  $\Delta t = 1$  year, as we want to measure the variation of the network structure in consecutive seasons. The similarity between partitions/covers is computed with the normalized mutual information, as usual. The similarity of two weighted networks like the ones at study is measured in the following way. First, one computes the distance  $d_{t,t+\Delta t}$  between the matrices  $\tilde{\mathbf{W}}^t$  and  $\tilde{\mathbf{W}}^{t+\Delta t}$ : 
$$d_{t,t+\Delta t} = \sqrt{\sum_{ij} (\tilde{W}_{ij}^t - \tilde{W}_{ij}^{t+\Delta t})^2}$$
. The matrix  $\tilde{\mathbf{W}}^t$  is derived from the standard weight matrix  $\mathbf{W}^t$  by dividing each edge weight by the sum of all edge weights. This is done because the traffic flows tend to increase steadily in time, so comparing the original weight matrices is not appropriate. The quantity  $d_{t,t+\Delta t}$  is a dissimilarity measure. We turn it to a similarity index by changing its sign, adding a constant and rescaling the resulting values. Since we wish to compare the trend of the network similarity with that of the partition/cover similarity, the additional constant and the rescaling factor are chosen such to reproduce the average and the variance of the curve of the normalized mutual information. After this operation, the two trends are finally comparable. The diagram shows that both measures follow a yearly periodicity, with peaks corresponding to the winter season, which is then more stable than the others.

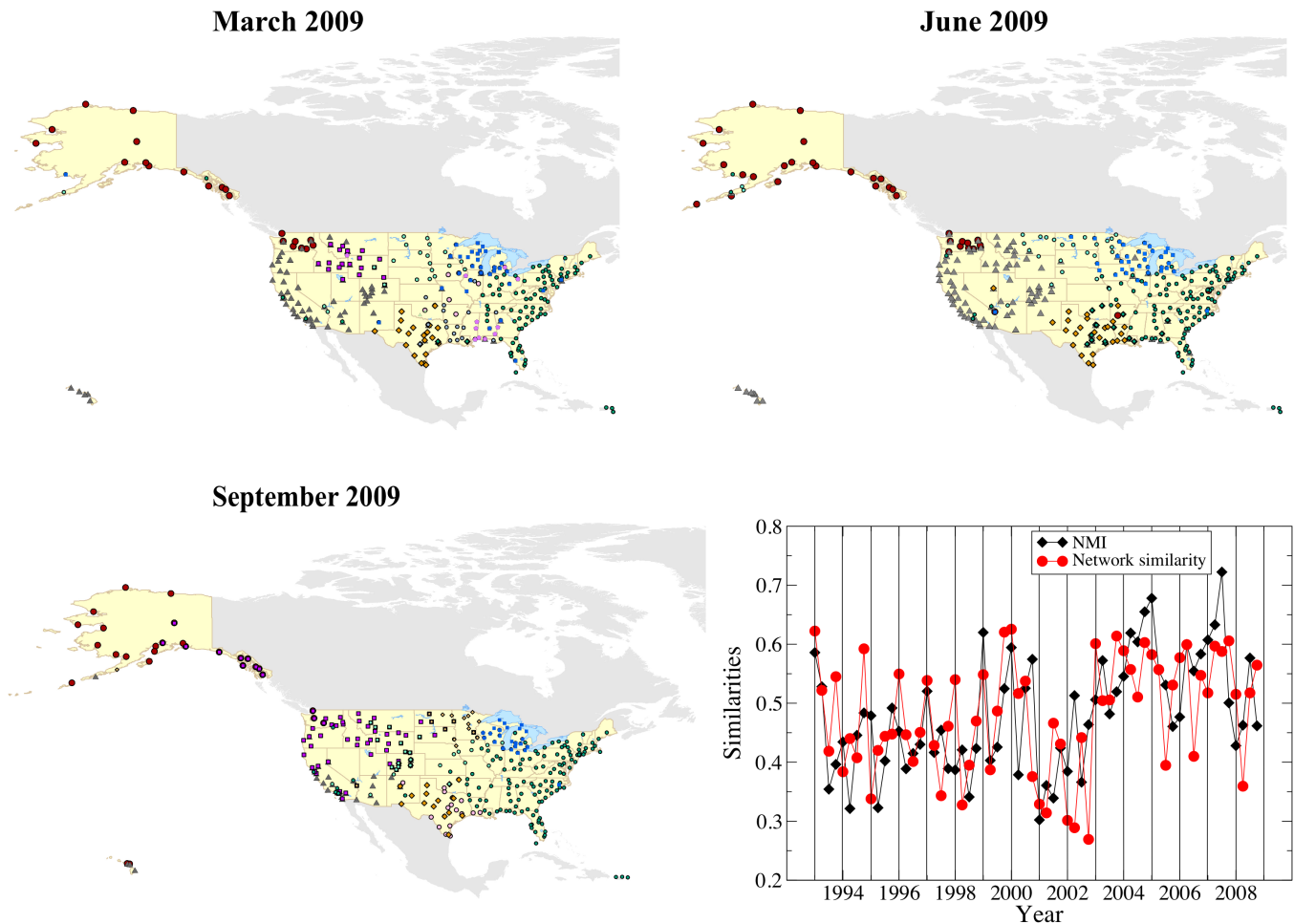


Figure 16: Application of OSLOM to real networks: US airport network. The maps show the position of the airports, which are represented by symbols, indicating the communities found by applying OSLOM directly to the corresponding network, without exploiting the information of previous snapshots. The diagram shows the “seasonality” of air traffic. The normalized mutual information (diamonds) was computed comparing the cover of the system at time  $t$  adjusted by OSLOM on the network at time  $t + \Delta t$ , and the cover obtained by applying OSLOM directly to the system at time  $t + \Delta t$ . The circles are estimates of the similarity of the network matrices of snapshots separated by  $\Delta t$  (one year). For each year we took four snapshots, by cumulating the traffic of each trimester. The most stable networks are typically in winter (vertical lines).

#### IV. DISCUSSION

We have introduced OSLOM, the first method that finds clusters in networks based on their statistical significance. It is a multi-purpose technique, capable to handle various types of graphs, accounting for edge direction, edge weights, overlapping communities, hierarchy and network dynamics. Therefore, it can be used for a wide variety of datasets and applications.

We have thoroughly tested OSLOM against the best algorithms currently available on various types of artificial benchmark graphs, with excellent results. In particular, OSLOM is superior on directed graphs and in the detection of strongly overlapping clusters. Moreover, it is an ideal method to recognize the absence of community structure and/or the presence of randomness in

graphs. In some cases OSLOM returns slightly less accurate results than other methods, because it finds several homeless vertices when communities are fuzzy. This is due to the fact that, in the realizations of benchmark graphs, it may happen that some vertices end up having the same number of neighbors (or even more) in other communities than in their own, due to fluctuations, even if on average this does not happen. So, the classification of those vertices, *imposed* by the planted  $\ell$ -partition model, is not justified topologically. This is an important general issue that needs to be assessed in the future, to avoid systematic errors in the testing procedure.

OSLOM is a local algorithm, so it respects the nature of community structure, which is a local feature of networks, the more so the larger the systems at study. However, the null model adopted to estimate the statis-



tical significance of clusters is the configuration model, which is global. This is the same null model adopted in modularity optimization [63], and is responsible for the serious problems of this technique, like its well known resolution limit [64]. Therefore we perform an iterative cluster search within the clusters found after the first application of the method, by considering each cluster as a network on its own. In this way we progressively limit the horizon of the part of the network under exploration, and we are able to find the smallest significant clusters, which are the natural building blocks of the network and the basis of its hierarchical community structure. So the null model, originally global, gets confined to smaller and smaller portions of the graph. The actual resolution of the method is thus not due to the null model, but to the choice of the threshold  $P$ . In this paper we have set  $P = 0.1$ , which is often used in various contexts and delivers an excellent performance on the benchmark graphs we have adopted. Nevertheless, how much a real graph *deviates* from a random graph depends on the specific system at hand, and it would be more appropriate to estimate the threshold  $P$  case by case. This is an issue to consider for future work. We remark that also for modularity optimization one could in principle iteratively restrict the null model to the clusters found by the method. However, modularity is based on the *expected* value of variables estimated on the null model, neglecting random fluctuations, which is why modularity can attain large values on specific partitions of random graphs [65–67]. OSLOM instead accounts for those fluctuations, so it is far more reliable, in this respect. Furthermore OSLOM is a local method, so it does not suffer from the severe problems coming from modularity’s global optimization [68].

Another important aspect to emphasize is the need to perform many iterations, to get more accurate results. This is not a specific feature of OSLOM, but it should be done for all community detection techniques with a stochastic character, like methods based on optimization (e. g., modularity optimization). In the literature there is the general attitude to perform a single iteration, and to reduce the complexity of an algorithm to the time required to carry out one iteration. But this is not appropriate, especially on large networks. For instance, by performing a single iteration, vertices lying on the border between clusters may be assigned to a specific cluster, while in many cases they are overlapping. By combining the results of several iterations, instead, it is more likely to distinguish overlapping vertices from the others. Furthermore, one can compute the strength of the membership of vertices in different clusters, from the frequency with which they were classified in each cluster. One can also disambiguate stable from unstable clusters, which could be recovered from specific iterations. So, it is crucial to collect and combine the results of many iterations. Of course, the complexity of the method grows with the number of iterations, but it can be considerably reduced by distributing runs among many different processors, if

large computer clusters are available.

The running time of OSLOM is dominated by the exhaustive search of significant vertices, inside and outside the clusters. This search could be carried out with greedy approaches, with a huge computational advantage, and this is an improvement we plan to implement in the near future. On the other hand, if one wishes to attack very large graphs, OSLOM could be used at a second stage, as a refinement technique, to clean the results of an initial partition delivered by a fast algorithm. In this case, since the initial clusters are usually cores or parts of the significant clusters we are looking for, OSLOM converges far more rapidly than its direct application without inputs. We have seen in the previous section that, by combining OSLOM with the Louvain method by Blondel et al., we were able to handle systems with millions of vertices.

We have proposed a recipe to deal with the increasingly more important issue of detecting communities in dynamic networks. The idea is to take advantage of the information of different snapshots at the same time, by “adapting” the partition/cover of the earlier snapshot to the topology of the other one. In this way it is possible to uncover the correlation between the structures of the system at different time stamps.

We have shown the versatility of OSLOM by applying it to various networked datasets. OSLOM provides the first comprehensive toolbox for the analysis of community structure in graphs and is an ideal complement of existing tools for network analysis. The algorithm, with all its variants (including a fast two-step procedure for the analysis of very large networks) is implemented in a freely downloadable and documented software (<http://www.oslom.org>).

## Acknowledgments

We thank Paolo Bajardi, Steve Gregory and Martin Rosvall for useful suggestions. A. L. and S. F. gratefully acknowledge ICTeCollective. The project ICTeCollective acknowledges the financial support of the Future and Emerging Technologies (FET) programme within the Seventh Framework Programme for Research of the European Commission, under FET-Open grant number 238597.

## Appendix A: Numerical estimation of the internal connection probability

The assessment of a cluster’s significance given the null (configuration) model relies on the estimation of the probability described in Eq. 1. This function has to be evaluated many times along the execution of OSLOM in order to clean up each cluster and to evaluate the clusters at the different hierarchical levels. We explain here how the values of the distribution function can be estimated or approximated in a practical implementation of

OSLOM.

For convenience, we rewrite the equation here

$$p(k_i^{in}|i, \mathcal{C}, \mathcal{G}) = A \frac{2^{-k_i^{in}}}{k_i^{out}! k_i^{in}! (m_{\mathcal{C}}^{out} - k_i^{in})! (M^*/2)!}. \quad (\text{A1})$$

While estimating the value of the probability of Eq. A1 for a certain  $k_i^{in}$ , the most computationally expensive part is the evaluation of the normalization factor  $A$ . In fact, this would force us to evaluate the rest of the formula for all the allowed values of  $k_i^{in}$  and add up the result. A simple way out of this problem is to approximate the distribution by another whose normalization factor is known. To do so, we can think of a slightly different null model, in which the edges are still drawn at random and the formation of self-loops is admitted. This is actually the null model on which the definition of modularity is based [40]. In such model, the equivalent of Eq. A1 becomes an hypergeometric function that is much easier to estimate (see [31]). Both distributions, that of Eq. A1 and the hypergeometric, provide close numerical values for the same  $k_i^{in}$ , except if the probability of generating self-loops in the null model is high. The probability that reshuffling the connections at random a stub of vertex  $i$  connects to another stub of the same vertex, is given by  $k_i^2/2M$ . In the software implementation of OSLOM, the hypergeometric approximation for Eq. A1 is used as long as  $k_i^2/2M < 1$ . Otherwise, we directly measure  $A$  from Eq. A1.

## Appendix B: Extension of the method to weighted networks

In the main text, it is briefly discussed how to extend OSLOM to weighted graphs. We mention also that some of the technical issues, such as combining both  $r_w$  and  $r_t$ , are not trivial. This procedure is described here in further detail.

Remember that we start from an ansatz for the distribution of the weights in the null model. The distribution of the probability of having a certain weight on the edge joining vertices  $i$  and  $j$  was assumed to be

$$p(w_{ij} > x | k_i, k_j, s_i, s_j) = \exp(-x/\langle w_{ij} \rangle). \quad (\text{B1})$$

The idea behind this expression is that the weight of an edge is proportional to the average weight of its endvertices ( $\langle w_i \rangle = s_i/k_i$  and  $\langle w_j \rangle = s_j/k_j$ ). We proposed the harmonic average because it is more sensitive to small values of  $\langle w_i \rangle$ . Our goal is to define a fitness function  $r$  which has to be a uniform random variable on our randomized weighted network. And we want to combine the fitness function depending on the topology with one depending on the weight distribution in order to detect meaningful fluctuations in any of them.

Let us consider a vertex  $i$  which has  $l$  connections with a given subgraph  $\mathcal{C}$  (not including  $i$ ). For the topological part, we have already computed the probability that  $i$

shares  $l$  or more edges with vertices of  $\mathcal{C}$  (Eq. A1). We call this number  $r_t$ . Each of the  $l$  edges joining  $i$  with  $\mathcal{C}$  carries a weight. We consider the corresponding normalized weight  $\omega_s = w_s/\langle w_s \rangle$ , where  $w_s$  is the weight on the  $s$ -th edge, with  $s = 1, 2, \dots, l$ . Since we want a single number taking into account all the weights in the set, we can simply consider the sum of all the  $\omega_s$ :

$$\Omega = \sum_{s=1}^l \omega_s \quad (\text{B2})$$

$\Omega$  is the sum of  $l$  exponentially distributed variables (with rate equal to one) and therefore it follows the Erlang distribution [69]. Let us call  $r_w$  the cumulative of  $\Omega$ :

$$r_w = p(\Omega > x) = e^{-x} \sum_{q=0}^{l-1} x^q/q! \quad (\text{B3})$$

In this way, we managed to define two variables  $r_t$  and  $r_w$  which are both uniformly distributed in the null model. Now, we would like to combine these two scores to have a final score for our vertex  $i$ . Unfortunately this is not so simple. We remind that  $r_w$  is defined only on the  $N_n$  neighbors of subgraph  $\mathcal{C}$  while  $r_t$  is defined for all the  $N^* = N - n_{\mathcal{C}} \geq N_n$  vertices out of  $\mathcal{C}$ , so the two variables are defined on samples of different size, in general. A way to overcome this difficulty is to scale  $r_t$  to an equivalent random variable  $r'_t$  defined on a smaller sample. This amounts to map each index  $i$  in the set  $1, 2, \dots, N^*$  of the old variable onto an index  $j$  in the set  $1, 2, \dots, N_n$  of the new variable. Given  $i$ , the natural solution is to pick the index  $j$  such that the cumulative probability  $\Omega_q^t$  on the sample of  $N^*$  vertices coincides (at least with the approximation allowed by the specific numerics involved) with the cumulative probability  $\Omega_q^w$  on the smaller sample of  $N_n$  vertices. It can be shown that this can be achieved with a good approximation (in the limit of  $j$  close to  $N_n$ ) with the following rescaling:

$$r'_t = r_t \cdot \frac{N^* + 1}{N_n + 1}. \quad (\text{B4})$$

Once we computed  $r'_t$  and  $r_w$  we need to combine them in order to have a single score to rank the vertices. We consider the product  $r'_t \cdot r_w$  and the final score  $r_{tw} = p(r'_t \cdot r_w < x) = x(1 - \log x)$ . The last expression comes from the assumption that the two variables are both uniform and independent. The set of variables  $\{r_{tw}\}$  is then used to rank the vertices and to compute the cumulative probabilities  $\Omega_q^{tw}$ , with  $N_n$  instead of  $N^*$ .

## Appendix C: Further tests on benchmark graphs

### 1. Girvan-Newman benchmark

The benchmark by Girvan and Newman [8] (GN benchmark) is a class of graphs with 128 vertices, each,

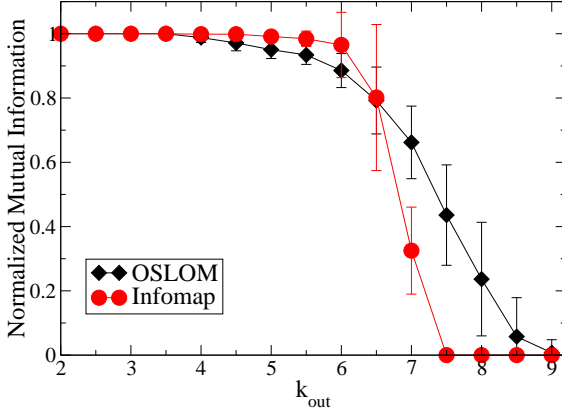


Figure 17: Test on the Girvan-Newman benchmark graphs. The variable  $k_{out}$  is the average number of external neighbors per vertex. The two curves refer to OSLOM (diamonds) and Infomap (circles).

divided into four equal-sized groups. Every vertex has expected degree 16 (with a very peaked distribution about 16). The (average) number of neighbors of a vertex within its group is  $k_{in}$ , whereas the (average) number of external neighbors is  $k_{out}$ . By construction,  $k_{in} + k_{out} = 16$ . In the language of the planted  $\ell$ -partition model [43], the probability that a vertex is linked to another vertex of its group is  $p = k_{in}/31$ , the probability that a vertex is linked to external vertices is  $q = k_{out}/96$ . The condition  $p > q$  for the four groups to be communities is then equivalent to  $k_{out} \lesssim 12$  (this does not account for random fluctuations, though [30, 31]).

Fig. 17 shows the Normalized Mutual Information (in the version devised in Ref. [23]) between the planted partition of the GN benchmark and the partition found by the algorithm as a function of  $k_{out}$ . As a term of comparison we used again Infomap [49]. Fig. 17 shows that Infomap is more accurate for low values of  $k_{out}$  than OSLOM, but its performance drops rapidly for  $k_{out} \gtrsim 6$ , whereas OSLOM shows a slower decay.

OSLOM is slightly worse than Infomap because it finds several homeless vertices, as we explained in the main text (Section III A 1).

## 2. Weighted LFR benchmark

In Figs. 18 and 19 we report the comparative analysis of OSLOM and Infomap on weighted LFR graphs. To build the weighted benchmark graphs [42] one needs two additional parameters: the exponent  $\beta$  of the relation between the strength of a vertex and its degree (the strength of a vertex is the sum of the weights of the edges incident on the vertex); the weighted mixing parameter

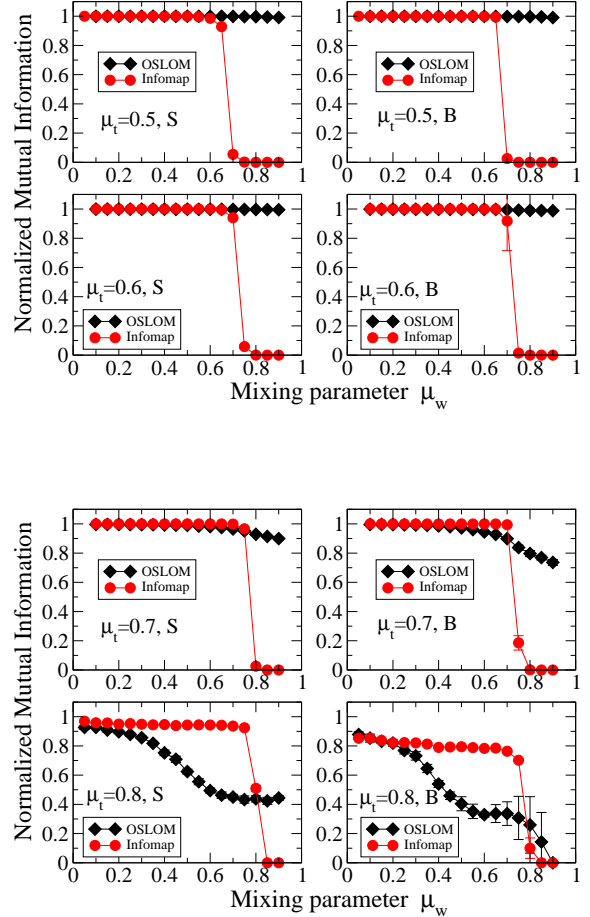


Figure 18: Test on weighted LFR benchmark graphs (undirected and without overlapping communities). The parameters are:  $N = 5000$ ,  $\langle k \rangle = 20$ ,  $k_{max} = 50$ ,  $\tau_1 = 2$ ,  $\tau_2 = 1$ ,  $\beta = 1.5$ . Each panel corresponds to a given value of the topological mixing parameter  $\mu_t$  and of the community range (S or B).

$\mu_w$ , which is the natural extension to weighted networks of the topological  $\mu$  (that here we call  $\mu_t$ ), i.e. it is the ratio between the sum of the weights on the edges joining a vertex to its neighbors in different communities and the strength of the vertex. In the analysis, we fix the value of the topological mixing parameter  $\mu_t$  and see how the normalized mutual information varies as a function of  $\mu_w$ . In Fig. 18 the benchmark graphs consist of 5000 vertices, and we consider the usual two ranges of community sizes (S and B). In Fig. 19 the graphs consist of 50000 vertices, and we consider a single, but much wider, range of community sizes (from 20 to 1000). When  $\mu_t = 0.5$  or  $\mu_t = 0.6$ , we find that OSLOM detects the right clusters for any value of  $\mu_w$ , for  $N = 5000$ , which is truly remarkable, while Infomap is unable to find the partition for  $\mu_w \gtrsim 0.6$ . OSLOM's striking result comes from the

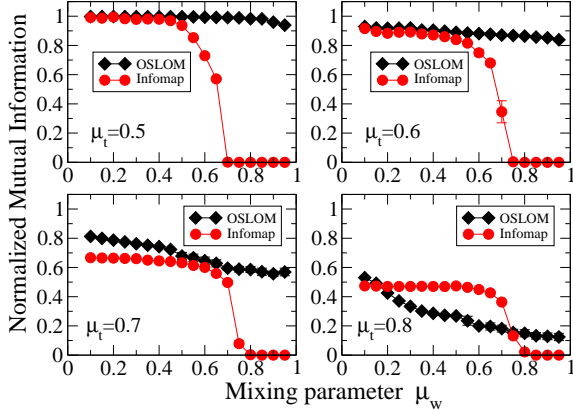


Figure 19: Test on weighted LFR benchmark graphs (undirected and without overlapping communities). The parameters are:  $N = 50000$ ,  $\langle k \rangle = 20$ ,  $k_{max} = 200$ ,  $\tau_1 = 2$ ,  $\tau_2 = 1$ ,  $\beta = 1.5$ . Each panel corresponds to a given value of the topological mixing parameter  $\mu_t$ . The range of community sizes is  $[20, 1000]$ .

fact that the score  $r_{tw}$  of a vertex on weighted graphs is given by the product of two numbers, the topological score  $r'_t$  and the weight score  $r_w$  (Section IID 5). If  $\mu_t$  is not too large, the topological term  $r'_t$  is very low and brings down the whole score  $r_{tw}$ , which remains significant for any choice of the weighted mixing parameter  $\mu_w$ . Basically, OSLOM is able to recognize the right clusters from the topology alone. When  $\mu_t = 0.5$  or  $\mu_t = 0.6$  and  $N = 50000$ , OSLOM maintains an excellent performance for the whole range of  $\mu_w$ , while Infomap again fails for  $\mu_w \gtrsim 0.6$ . For  $\mu_t = 0.7$  the performances of the two algorithms worsen and OSLOM is still superior, though the results are essentially comparable for both network sizes. For  $\mu_t = 0.8$  Infomap is more accurate than OSLOM, when  $N = 5000$ , while both methods are not very good when  $N = 50000$ . However, from Figs. 18 and 19 it is apparent that OSLOM works the better, the larger the network size. So, on very large networks ( $N \gg 50000$ ) we expect that OSLOM has a comparable or superior performance than Infomap for every pair of values  $(\mu_t, \mu_w)$ . We also infer that the performance of both algorithms worsens if clusters are on average larger.

### 3. Directed LFR benchmark

Figs. 20 and 21 show the results of the test on directed LFR graphs [42]. This time we have to distinguish between in-degree (number of incoming edges) and out-degree (number of outgoing edges) of a vertex. The in-degree distribution is taken to be a power law, with exponent  $\tau_{in}$ , whereas the out-degree is the same

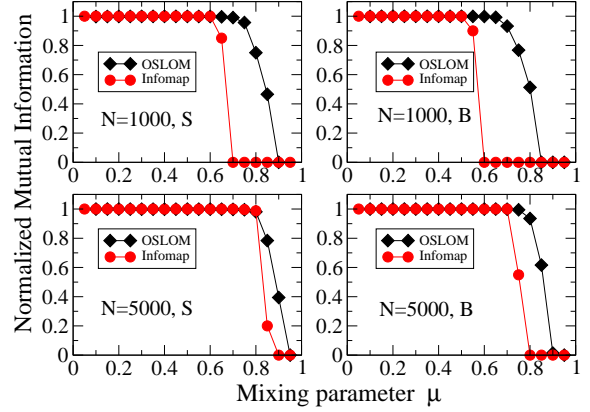


Figure 20: Test on directed LFR benchmark graphs (unweighted and without overlapping communities). The parameters are:  $\langle k \rangle = 20$ ,  $k_{max} = 50$ ,  $\tau_{in} = 2$ ,  $\tau_2 = 1$ . Each panel corresponds to a given network size ( $N = 1000, 5000$ ) and community range (S or B). The mixing parameter  $\mu$  refers to in-degree.

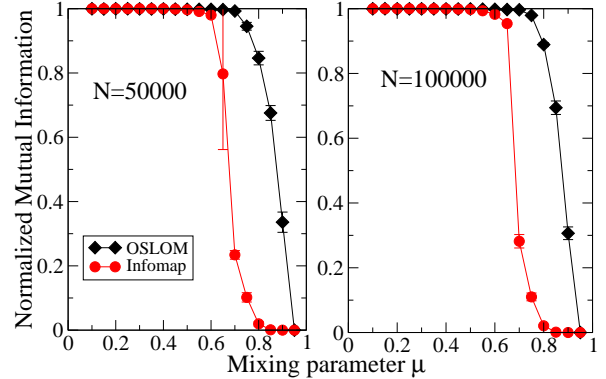


Figure 21: Test on directed LFR benchmark graphs (unweighted and without overlapping communities). The parameters are:  $\langle k \rangle = 20$ ,  $k_{max} = 200$ ,  $\tau_{in} = 2$ ,  $\tau_2 = 1$ . We consider two large network sizes:  $N = 50000$  (left) and  $N = 100000$  (right). The range of community sizes is  $[20, 1000]$ . The mixing parameter  $\mu$  refers to in-degree.

for all vertices, for simplicity. The mixing parameter  $\mu$  expresses the ratio of the number of in-neighbors of a vertex belonging to different clusters and the total number of in-neighbors of the vertex. The in-neighbor of a vertex  $i$  is any vertex  $j$  connected to  $i$  by an edge going from  $j$  to  $i$ . Figs. 20 and 21 tell us that OSLOM outperforms Infomap, especially when communities span a

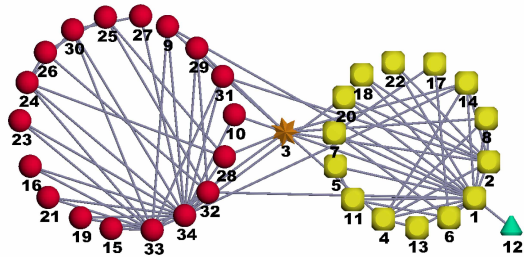


Figure 22: Application of OSLOM to real networks: Zachary's karate club.

broader range of sizes. The performances of both algorithms slightly worsen on larger networks.

## Appendix D: Real-world systems

### 1. Zachary karate club

The famous karate club network of Zachary [70] is a standard benchmark in community detection. Vertices are members of a karate club in the United States, who were monitored during a period of three years. Edges connect members who had social interactions outside the club. After some time, a conflict between the club president and the instructor caused the fission of the club in two separate groups, supporting the instructor and the president, respectively. In Fig. 22 we see the community structure found by OSLOM. It indeed finds two communities, plus a homeless vertex (12). Vertex 3 is shared between the two clusters, as it has several neighbors in both groups. We shall illustrate overlapping and homeless vertices with stars and triangles, respectively. The communities coincide with the ones observed by Zachary with the exception of vertices 3 and 12, which Zachary put with the squares. However, vertex 3 is overlapping, so it belongs to both clusters, which seems quite reasonable by looking at the figure. Also, vertex 12 is homeless due to its loose relationship with its group (it has only one neighbor).

### 2. Dolphin social network

Fig. 23 presents OSLOM's results for the network of bottlenose dolphins living in Doubtful Sound (New

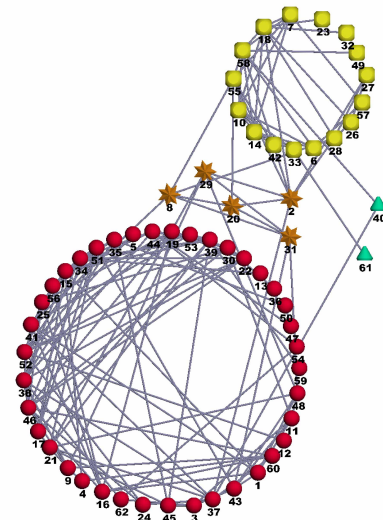


Figure 23: Application of OSLOM to real networks: Lusseau's social network of bottlenose dolphins.

Zealand). The network was compiled by Lusseau [71]. Vertices of the network are dolphins and two dolphins are connected if they were seen together more often than expected by chance. The dolphins separated in two groups after one of them left the place for some time. OSLOM finds two communities, with five overlapping vertices (2, 8, 20, 29, 31), plus two homeless vertices (40, 61), which are very loosely connected to the rest of the graph. All vertices which are uniquely assigned to the same group (indicated by the same symbol, square or circle, in the figure) are classified in the same community by Lusseau as well.

### 3. American college football

Another well known benchmark in community detection is the network of American college football teams, compiled by Girvan and Newman [8]. It comprises 115 vertices, representing Division I-A colleges. Edges correspond to games played by the teams against each other during the regular season of fall 2000. The teams are divided into 12 conferences. Games between teams in the same conference are usually (but not always) more frequent than games between teams of different conferences, so there is an organization in clusters where communities correspond to conferences. In Fig. 24 we see that OSLOM finds three hierarchical levels. The lowest level consists of 11 clusters and 5 homeless vertices. There are no overlapping vertices. Six clusters correspond exactly to the conferences, three others match the conferences up to one vertex, one up to two vertices, the last cluster along with the homeless vertices mostly mix teams of the conferences Sun Belt and Independents. The latter is not a proper conference, whereas Sun Belt includes colleges

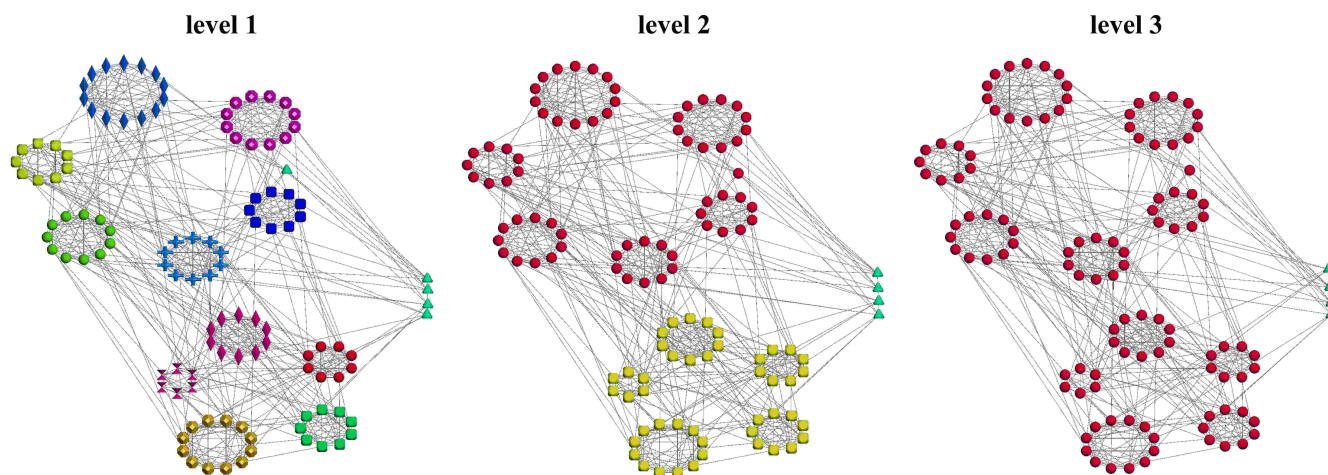


Figure 24: Application of OSLOM to real networks: American college football network.

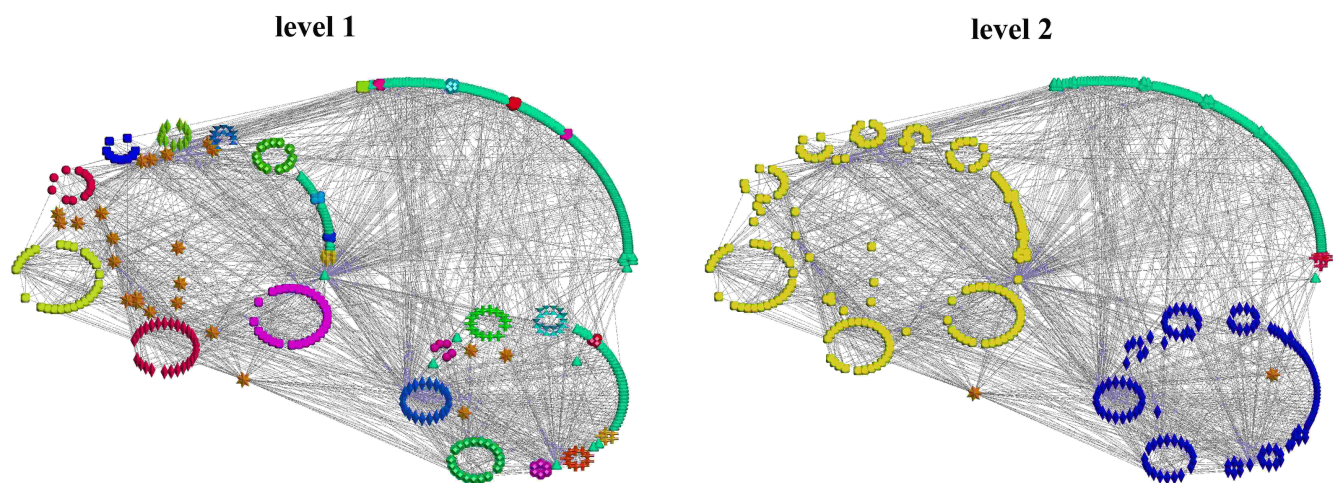


Figure 25: Application of OSLOM to real networks: metabolic network of *C. elegans*.

which are geographically very spreadout, so they happen to play quite often games with the other teams, resulting much more mixed with them than teams of other conferences. Interestingly, in the second hierarchical level we find two large communities (plus four homeless teams), corresponding quite well to a geographical separation of the colleges in East and West.

#### 4. *C. elegans* metabolic network

Fig. 25 presents the community structure of the metabolic network of *C. elegans*. The network has been compiled by Duch and Arenas [72] and it has been often used in applications of community detection algorithms. Vertices are metabolites and edges connect pairs

of metabolites involved in at least one biochemical reaction. OSLOM finds two hierarchical levels, the lower with 25 clusters, the higher with 3 (but one of them is much smaller than the other two). The fraction of homeless vertices in the lower level is larger than 20% (see Table 1) and the network appears rather “noisy”.

- [1] R. Albert and A.-L. Barabási, *Rev. Mod. Phys.*, **74**, 47 (2002).
- [2] S. N. Dorogovtsev and J. F. F. Mendes, *Adv. Phys.*, **51**, 1079 (2002).
- [3] M. E. J. Newman, *SIAM Rev.*, **45**, 167 (2003).
- [4] R. Pastor-Satorras and A. Vespignani, *Evolution and Structure of the Internet: A Statistical Physics Approach* (Cambridge University Press, New York, NY, USA, 2004).
- [5] S. Boccaletti, V. Latora, Y. Moreno, M. Chavez, and D. U. Hwang, *Phys. Rep.*, **424**, 175 (2006).
- [6] A. Barrat, M. Barthélemy, and A. Vespignani, *Dynamical processes on complex networks* (Cambridge University Press, Cambridge, UK, 2008).
- [7] G. Caldarelli, *Scale-free networks* (Oxford University Press, Oxford, UK, 2007).
- [8] M. Girvan and M. E. J. Newman, *Proc. Natl. Acad. Sci. USA*, **99**, 7821 (2002).
- [9] D. Lusseau and M. E. J. Newman, *Proc. Royal Soc. London B*, **271**, S477 (2004).
- [10] L. A. Adamic and N. Glance, in *LinkKDD '05: Proceedings of the 3rd international workshop on Link discovery* (ACM Press, New York, NY, USA, 2005) pp. 36–43, ISBN 1595932151.
- [11] G. W. Flake, S. Lawrence, C. Lee Giles, and F. M. Coetzee, *IEEE Computer*, **35**, 66 (2002).
- [12] S. L. Pimm, *Theor. Popul. Biol.*, **16**, 144 (1979).
- [13] A. E. Krause, K. A. Frank, D. M. Mason, R. E. Ulanowicz, and W. W. Taylor, *Nature*, **426**, 282 (2003).
- [14] P. F. Jonsson, T. Cavanna, D. Zicha, and P. A. Bates, *BMC Bioinf.*, **7**, 2 (2006).
- [15] P. Holme, M. Huss, and H. Jeong, *Bioinformatics*, **19**, 532 (2003).
- [16] R. Guimerà and L. A. N. Amaral, *Nature*, **433**, 895 (2005).
- [17] S. Fortunato, *Phys. Rep.*, **486**, 75 (2010).
- [18] J. Baumes, M. K. Goldberg, M. S. Krishnamoorthy, M. M. Ismail, and N. Preston, in *IADIS AC*, edited by N. Guimaraes and P. T. Isaias (IADIS, 2005) pp. 97–104.
- [19] G. Palla, I. Derényi, I. Farkas, and T. Vicsek, *Nature*, **435**, 814 (2005).
- [20] S. Zhang, R.-S. Wang, and X.-S. Zhang, *Physica A*, **374**, 483 (2007).
- [21] S. Gregory, in *Proceedings of the 11th European Conference on Principles and Practice of Knowledge Discovery in Databases (PKDD 2007)* (Springer-Verlag, Berlin, Germany, 2007) pp. 91–102.
- [22] T. Nepusz, A. Petróczy, L. Négyessy, and F. Bazsó, *Phys. Rev. E*, **77**, 016107 (2008).
- [23] A. Lancichinetti, S. Fortunato, and J. Kertész, *New J. Phys.*, **11**, 033015 (2009).
- [24] T. S. Evans and R. Lambiotte, *Phys. Rev. E*, **80**, 016105 (2009).
- [25] I. A. Kovács, R. Palotai, M. S. Szalay, and P. Csermely, *PLoS ONE*, **5**, e12528 (2010).
- [26] H. Simon, *Proc. Am. Phil. Soc.*, **106**, 467 (1962).
- [27] M. Sales-Pardo, R. Guimerà, A. A. Moreira, and L. A. N. Amaral, *Proc. Natl. Acad. Sci. USA*, **104**, 15224 (2007).
- [28] A. Clauset, C. Moore, and M. E. J. Newman, in *Statistical Network Analysis: Models, Issues, and New Directions*, *Lect. Notes Comp. Sci.*, Vol. 4503, edited by E. M. Airoldi, D. M. Blei, S. E. Fienberg, A. Goldenberg, E. P. Xing, and A. X. Zheng (Springer, Berlin, Germany, 2007) pp. 1–13.
- [29] A. Clauset, C. Moore, and M. E. J. Newman, *Nature*, **453**, 98 (2008).
- [30] G. Bianconi, P. Pin, and M. Marsili, *Proc. Natl. Acad. Sci. USA*, **106**, 11433 (2009).
- [31] A. Lancichinetti, F. Radicchi, and J. J. Ramasco, *Phys. Rev. E*, **81**, 046110 (2010).
- [32] J. Hopcroft, O. Khan, B. Kulis, and B. Selman, *Proc. Natl. Acad. Sci. USA*, **101**, 5249 (2004).
- [33] L. Backstrom, D. Huttenlocher, J. Kleinberg, and X. Lan, in *KDD '06: Proceedings of the 12th ACM SIGKDD international conference on Knowledge discovery and data mining* (ACM, New York, NY, USA, 2006) pp. 44–54.
- [34] D. Chakrabarti, R. Kumar, and A. Tomkins, in *KDD '06: Proceedings of the 12th ACM SIGKDD international conference on Knowledge discovery and data mining* (ACM, New York, NY, USA, 2006) pp. 554–560.
- [35] G. Palla, A.-L. Barabási, and T. Vicsek, *Nature*, **446**, 664 (2007).
- [36] S. Asur, S. Parthasarathy, and D. Ucar, in *KDD '07: Proceedings of the 13th ACM SIGKDD international conference on Knowledge discovery and data mining* (ACM, New York, NY, USA, 2007) pp. 913–921.
- [37] P. J. Mucha, T. Richardson, K. Macon, M. A. Porter, and J. Onnela, *Science*, **328**, 876 (2010).
- [38] F. Radicchi, A. Lancichinetti, and J. J. Ramasco, *Phys. Rev. E*, **82**, 026102 (2010).
- [39] M. Molloy and B. Reed, *Random Struct. Algor.*, **6**, 161 (1995).
- [40] M. E. J. Newman and M. Girvan, *Phys. Rev. E*, **69**, 026113 (2004).
- [41] A. Lancichinetti, S. Fortunato, and F. Radicchi, *Phys. Rev. E*, **78**, 046110 (2008).
- [42] A. Lancichinetti and S. Fortunato, *Phys. Rev. E*, **80**, 016118 (2009).
- [43] A. Condon and R. M. Karp, *Random Struct. Algor.*, **18**, 116 (2001).
- [44] R. Albert, H. Jeong, and A.-L. Barabási, *Nature*, **406**, 378 (2000).
- [45] M. E. J. Newman, *Eur. Phys. J. B*, **38**, 321 (2004).
- [46] F. Radicchi, C. Castellano, F. Cecconi, V. Loreto, and D. Parisi, *Proc. Natl. Acad. Sci. USA*, **101**, 2658 (2004).
- [47] A. Clauset, M. E. J. Newman, and C. Moore, *Phys. Rev. E*, **70**, 066111 (2004).
- [48] A. Lancichinetti, M. Kivela, J. Saramaki, and S. Fortunato, *PLoS ONE*, **5**, e11976 (2010).
- [49] M. Rosvall and C. T. Bergstrom, *Proc. Natl. Acad. Sci. USA*, **105**, 1118 (2008).
- [50] A. Lancichinetti and S. Fortunato, *Phys. Rev. E*, **80**, 056117 (2009).
- [51] L. Danon, A. Díaz-Guilera, J. Duch, and A. Arenas, *J. Stat. Mech.*, **P09008** (2005).
- [52] S. Gregory, *New J. Phys.*, **12**, 103018 (2010).
- [53] U. N. Raghavan, R. Albert, and S. Kumara, *Phys. Rev. E*, **76**, 036106 (2007).
- [54] A. McDaid and N. J. Hurley, in *ASONAM 2010* (2010).
- [55] K. Nowicki and T. A. B. Snijders, *J. Am. Stat. Assoc.*, **96** (2001).

- [56] M. Rosvall and C. T. Bergstrom, Eprint arXiv:1010.0431 (2010).
- [57] P. Erdős and A. Rényi, *Publ. Math. Debrecen*, **6**, 290 (1959).
- [58] A.-L. Barabási and R. Albert, *Science*, **286**, 509 (1999).
- [59] P.-N. Tan, M. Steinbach, and V. Kumar, *Introduction to Data Mining*, 1st ed. (Addison Wesley, New York, USA, 2005).
- [60] D. L. Nelson, C. L. McEvoy, and T. A. Schreiber, “The university of south florida word association, rhyme, and word fragment norms,” (1998).
- [61] V. D. Blondel, J.-L. Guillaume, R. Lambiotte, and E. Lefebvre, *J. Stat. Mech.*, **P10008** (2008).
- [62] I. X. Y. Leung, P. Hui, P. Liò, and J. Crowcroft, *Phys. Rev. E*, **79**, 066107 (2009).
- [63] M. E. J. Newman, *Proc. Natl. Acad. Sci. USA*, **103**, 8577 (2006).
- [64] S. Fortunato and M. Barthélemy, *Proc. Natl. Acad. Sci. USA*, **104**, 36 (2007).
- [65] R. Guimerà, M. Sales-Pardo, and L. A. Amaral, *Phys. Rev. E*, **70**, 025101 (R) (2004).
- [66] J. Reichardt and S. Bornholdt, *Physica D*, **224**, 20 (2006).
- [67] J. Reichardt and S. Bornholdt, *Phys. Rev. E*, **76**, 015102 (R) (2007).
- [68] B. H. Good, Y.-A. de Montjoye, and A. Clauset, *Phys. Rev. E*, **81**, 046106 (2010).
- [69] M. Evans, N. Hastings, and B. Peacock, *Statistical Distributions* (Wiley-Interscience, New York, 2000).
- [70] W. W. Zachary, *J. Anthropol. Res.*, **33**, 452 (1977).
- [71] D. Lusseau, *Proc. Royal Soc. London B*, **270**, S186 (2003).
- [72] J. Duch and A. Arenas, *Phys. Rev. E*, **72**, 027104 (2005).